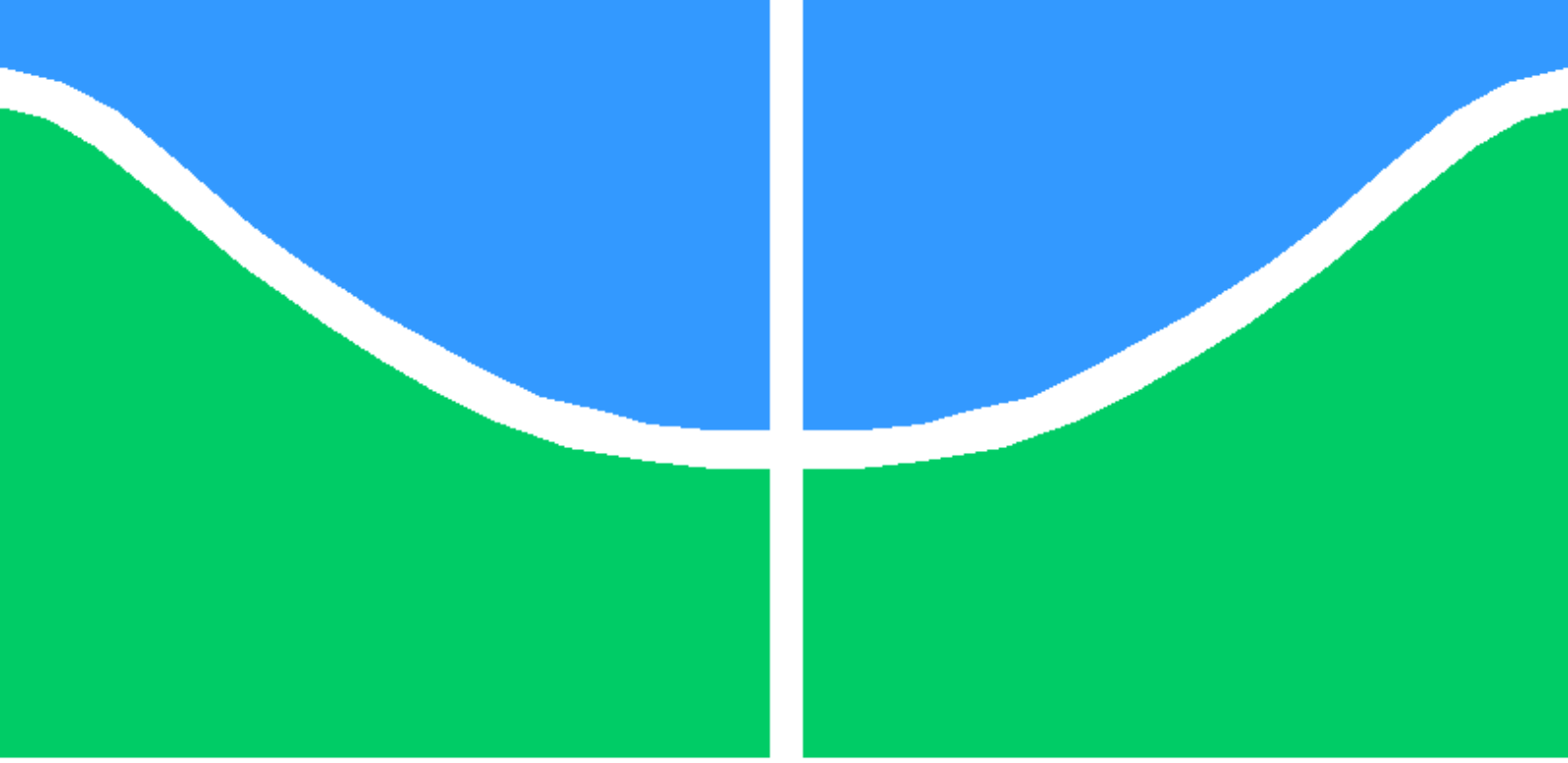

FLAT START GUESS HOMOTOPY-BASED POWER FLOW METHOD GUIDED BY FICTITIOUS NETWORK COMPENSATION CONTROL

ALISSON LIMA SILVA

DISSERTAÇÃO DE MESTRADO EM ENGENHARIA ELÉTRICA
DEPARTAMENTO DE ENGENHARIA ELÉTRICA

FACULDADE DE TECNOLOGIA

UNIVERSIDADE DE BRASÍLIA

UNIVERSIDADE DE BRASÍLIA
FACULDADE DE TECNOLOGIA
DEPARTAMENTO DE ENGENHARIA ELÉTRICA

FLAT START GUESS HOMOTOPY-BASED POWER FLOW METHOD GUIDED BY FICTITIOUS NETWORK COMPENSATION CONTROL

ALISSON LIMA SILVA

Orientador: PROF. DR. FRANCISCO DAMASCENO FREITAS, ENE/UNB

DISSERTAÇÃO DE MESTRADO EM ENGENHARIA ELÉTRICA

PUBLICAÇÃO PPGENE.DM - 782/22
BRASÍLIA-DF, 09 DE MAIO DE 2022.

UNIVERSIDADE DE BRASÍLIA
FACULDADE DE TECNOLOGIA
DEPARTAMENTO DE ENGENHARIA ELÉTRICA

FLAT START GUESS HOMOTOPY-BASED POWER FLOW METHOD GUIDED BY FICTITIOUS NETWORK COMPENSATION CONTROL

ALISSON LIMA SILVA

DISSERTAÇÃO DE MESTRADO ACADÊMICO SUBMETIDA AO DEPARTAMENTO DE ENGENHARIA ELÉTRICA DA FACULDADE DE TECNOLOGIA DA UNIVERSIDADE DE BRASÍLIA, COMO PARTE DOS REQUISITOS NECESSÁRIOS PARA A OBTENÇÃO DO GRAU DE MESTRE EM ENGENHARIA ELÉTRICA.

APROVADA POR:

Prof. Dr. Francisco Damasceno Freitas, ENE/UnB
Orientador

Prof. Dr. Kleber Melo e Silva, ENE/UnB
Examinador interno

Profa. Dra. Larissa Marques Peres, IFG-GO
Examinadora externa

Prof. Dr. Fernando Cardoso Melo, ENE/UnB
Examinador suplente

BRASÍLIA, 09 DE MAIO DE 2022.

FICHA CATALOGRÁFICA

LIMA-SILVA, ALISSON

Flat Start Guess Homotopy-based Power Flow Method Guided by Fictitious Network Compensation Control [Distrito Federal] 2022.

2022xiv, 67p., 210x297 mm (ENE/FT/UnB, Mestre, Engenharia Elétrica, 2022)

Dissertação de Mestrado - Universidade de Brasília

Faculdade de Tecnologia - Departamento de Engenharia Elétrica

1. Método da homotopia	2. Problema de fluxo de carga
3. Método de Newton-Raphson	4. Admitância shunt
5. Rede fictícia	6. Estimativa inicial padrão
7. MATPOWER	
I. ENE/FT/UnB	II. Título (série)

REFERÊNCIA BIBLIOGRÁFICA

Lima-Silva, A. (2022). Flat Start Guess Homotopy-based Power Flow Method Guided by Fictitious Network Compensation Control. Dissertação de Mestrado em Engenharia Elétrica, Publicação 782/22, Departamento de Engenharia Elétrica, Universidade de Brasília, Brasília, DF, 67p.

CESSÃO DE DIREITOS

AUTOR: Alisson Lima Silva

TÍTULO: Flat Start Guess Homotopy-based Power Flow Method Guided by Fictitious Network Compensation Control.

GRAU: Mestre ANO: 2022

_____

Alisson Lima Silva

Brasília-DF

Agradecimentos

Agradeço primeiramente a Deus pela saúde e pelas valiosas oportunidades que tem colocado em meu caminho.

A minha noiva Emília pelo amor, companheirismo, inspiração para seguir evoluindo na vida profissional e por tornar meus dias mais leves e felizes.

A minha mãe Denice e tia Dirce pelo carinho.

A UnB e ao Departamento de Engenharia Elétrica em especial ao professor Dr. Francisco Damasceno pelo apoio incondicional, sempre atencioso e solícito no desenvolvimento do trabalho.

Por fim, aos professores Dr. Kleber Melo e Dra. Larissa Marques por disponibilizarem seu tempo em contribuir com este trabalho.

Resumo

Este trabalho apresenta um método baseado em homotopia para o cálculo de soluções do Problema de Fluxo de Potência (PFP) partindo de uma estimativa inicial padrão, do tipo *flat start*. Este método de Solução Orientada por Homotopia - Newton-Raphson (GSH-NR) utiliza apenas a técnica de Newton-Raphson padrão para calcular as soluções fictícias ao longo do caminho da homotopia. A metodologia consiste em estruturar as equações do PFP durante o processo de homotopia para incorporar uma rede fictícia com elementos de admitância shunt para solução do problema. Além das admitâncias, um fator de escala é introduzido para fortalecer as interconexões próximas ao barramento de referência enquanto a homotopia é processada. Tanto as admitâncias shunt quanto o fator de escala são removidos completamente ao final do processo de homotopia. A vantagem da estratégia proposta é que o PFP é sempre resolvido partindo de uma estimativa inicial padrão e utilizando o método tradicional de NR ao longo das fases intermediárias do processo de homotopia. Para demonstrar a eficácia da técnica em encontrar a solução correta para o PFP, as simulações foram realizadas considerando vários modelos de sistemas de potência, incluindo um modelo tutorial e um sistema de grande porte com 70.000 barras.

Palavras-Chave: Método da homotopia; Problema de fluxo de carga; Método de Newton-Raphson; Admitância shunt; Rede fictícia; Estimativa inicial padrão; MATPOWER.

Abstract

This work presents a homotopy-based method to calculate the solution of a power flow problem (PFP) starting from a flat initial guess. This Guided Solution by Homotopy - Newton-Raphson (GSH-NR) method uses only the standard NR technique to compute the PFP fictitious states along the homotopy path. The methodology consists of structuring the PFP equations during the homotopy process to incorporate a fictitious additional network with shunt admittances to solve the problem. In addition to the admittances, a scaling factor is also introduced for strengthening the interconnections at the boundary of the slack bus while the homotopy is in progress. Both shunt admittances and the scaling factor are entirely removed at the end of the homotopy process. The advantage of the proposed strategy is that the PFP is always resolved by departing from a flat start estimate and using the traditional NR method along the intermediate stages of the homotopy procedure. To demonstrate the efficacy of the technique in finding an effective solution to the PFP, simulations are accomplished considering several system models, including a tutorial system and a large-scale system with 70,000 buses.

Keywords: Homotopy method; power flow problem; Newton-Raphson method; shunt admittance; fictitious network; flat start; MATPOWER.

CONTENTS

LIST OF FIGURES

LIST OF TABLES

LIST OF SYMBOLS AND ABBREVIATIONS

List of Symbols

α	Runge-Kutta's step parameter, usually defined as h
$\bar{\mathbf{x}}^{(k)}$, $\bar{\mathbf{x}}_0^{(k)}$	Converged state and initial estimate for the state $\mathbf{x}$ at the path point k
$\bar{Y}_{kk}$	kth diagonal entry of the original admittance matrix $\mathbf{Y}$
$\Delta\mathbf{x}^{(i)}$	Mismatch
Δh_1	Constant step adopted along the discrete computation of the homotopy path
Δh_1^{min}	Minimum step acceptable to discretize h_1
δ	Scaling factor used to change the impedance at a neighborhood of the slack bus
ϵ	Solution error
$\gamma(t)$	Homotopy path curve in function of a homotopy parameter t
$\hat{\mathbf{Y}}$	Modified admittance matrix
$\hat{y}_{km}$	Modified branch admittance at neighborhood of the slack bus
$\nabla_{\mathbf{x}}(\cdot)$	gradient operator of $(\cdot)$ for the variable $\mathbf{x}$
Ω_s	Set of buses composing a reduced region adjacent to the slack bus
Ω_{PQ}	Set of PQ buses
Ω_{PV}	Set of PV buses
$\overline{Y}_{km}$	Complex-valued element of bus admittance matrix
θ_{km}	Angular difference between θ_k and θ_m at buses $\#k$ and $\#m$
θ_k	Voltage angle at bus $\#k$

θ_m	Voltage angle at bus $\#m$
$\mathbf{f}(\mathbf{x})$	Compact notation for the set of nonlinear equations
$\mathbf{G}_x$	Jacobian matrix of the homotopy problem
$\mathbf{h}$	Homotopy continuation parameter set
$\mathbf{J}(\mathbf{x}^{(i)})$	Jacobian matrix
$\mathbf{x}$	Network state
$\mathbf{x}_{new}^{(h1,h2)}$	Converged solution in the search of the homotopy path
$\mathbf{x}_{old}^{(h1,h2)}$	Initial estimate to find a closer solution $\mathbf{x}_{new}^{(h1,h2)}$
b_k	Imaginary part of compensation shunt admittance at bus $\#k$
B_{km}	Imaginary part of $\overline{Y}_{km}$
g_k	Real part of compensation shunt admittance at bus $\#k$
G_{km}	Real part of $\overline{Y}_{km}$
h_1	Homotopy parameter used to control the inclusion and removal of the fictitious shunt admittance connected at buses PQ and PV
h_2	Homotopy parameter used to modify the admittances of the branches connecting buses in the region Ω_s
$iter$	Iteration number
max_{iter}	Maximum number of iterations
N_b	Number of buses
n_h	Number of continuation parameter
N_{PQ}	Number of PV bus
N_{PV}	Number of PQ bus
P_k	Net active power injected into bus $\#k$
Q_k	Net reactive power injected into bus $\#k$
t_{CPU}	Computational execution time
V_0	Voltage at slack bus
y_k	Compensation shunt admittance at bus $\#k$

List of Abbreviations

AC	Alternating Current
BE	Backward Euler
CFP	Continuation Power Flow Problem
CNM	Continuous Newton's Method
CPU	Central Processing Unit
DCPF	Direct Current Power Flow
EPE	Empresa de Pesquisa Energética
FE	Forward Euler method
GB	Gigabyte
Gen	Generation
GHz	Gigahertz
GS	Gauss-Seidel
GSH-NR	Guided Solution by Homotopy - Newton-Raphson
HV	High Voltage
ICNM	Implicit Continuous Newton's Method
IEEE	Institute of Electrical and Electronics Engineers
IH	Injection Homotopy
LV	Low Voltage
NR	Newton-Raphson
OPF	Optimal Power Flow
OS	Operating System
PBEs	Power Balance Equations
PDE	Partial Differential Equation
PFP	Power Flow Problem
PQ	Load Bus
pu	Per Unit

PV	Generations Bus
RAM	Random-access Memory
RK4	Runge-Kutta fourth-order method
RTE	Réseau de Transport de l'Electricité
SSD	Solid-state Drive
TWh	Terawatt hour

Chapter 1

Introduction

1.1 Overview

The Brazilian electrical system, like any other in general, undergoes constant changes aiming at its expansion. Projections of the Brazilian Energy Research Company (*Empresa de Pesquisa Energética - EPE*), in the reference scenario from 2021 to 2031 the sector should have an average growth of 3.5% annually. The development leads to an average annual growth of 22.9 TWh along the period [1].

Given the indicative character of the generation expansion, the process of elaboration of the system operation and expansion studies recognizes the importance of the role of the planned transmission network. A study of this nature must provide, in addition to adequate conditions of operation reliability and electrical supply, also the flexibility to accommodate different deployment strategies of generation sources. To this end, the initial survey of the power grid is carried out by the analysis of performance on a steady state in the various load levels and generation dispatch scenarios, by simulations of normal and non-simultaneous power flows of network elements.

Knowing that the supply of electricity is a joint effort between generation, transmission and distribution, the improvement and reduction of losses become a constant search. The inherent non-linearity of the power grid presents a great challenge to analyze its dynamic behaviors when subjected to disturbances, especially when a large amount of intermittent renewable energy is inserted. Identifying a stable equilibrium point of the dynamic system can significantly improve the operation of the system and therefore will be of great importance to avoid blackouts [2].

The study of the Power Flow Problem (PFP) has aroused the interest of researchers since its inception. Improving the reliability of nonlinear solutions has been the subject of research for decades [3]. This is a nonlinear problem that is of fundamental importance for determining the operating point of electrical power networks [4]. Its solution provides the equilibrium point of the network, which allows for obtaining other information, such as power flows in

interconnections, power produced in the power stations and the operational limits of the equipment. Thus, it becomes an essential tool for analyzing the operation of electrical power systems, evaluating the power system stability status and other applications, such as planning the expansion of the networks.

The traditional and widely accepted technique for solving PFP is the Newton-Raphson (NR) method [4, 5, 6, 7]. Other variants of the NR method are employed according to the simplification allowed for the network configuration. On the other hand, the NR presents local convergence and is sensitive to the initial estimate since it characterizes how close the guess is to the nonlinear problem solution. Therefore, physical factors such as loading conditions, network dimensions, and the number of iterations for ill- and well-conditioned cases affect the performance of the technique to solve the PFP [8]. According to [7], an ill-conditioned power system can be characterized as one which, although its solution does exist, is not solvable by using the standard NR technique and a flat start guess.

A flat start initialization is characterized by nominal voltages in the load buses and specified voltages in controlled buses (generation buses). Besides, all voltage phase angles are null. On the other hand, the flat start is a practical procedure to consider PFP initialization when an estimate at the boundary of the solution is distant or absent [4]. It is well known that the NR method presents quadratic convergence for an estimate inside the convergence region and at the neighborhood of the solution. These aspects involving the traditional NR method and its computational limitations motivated the investigation in the present work. The interest is in using it and in overcoming its deficiencies, even by departing from a flat start guess. To overcome these drawbacks, the combination of the NR method with a homotopy approach suggests an appropriate possibility to develop a hybrid approach, especially for large-scale systems.

Historically, the homotopy theorem was first proposed by Witold Hurewicz in 1935 [9]. Over the years, it has been applied to solve nonlinear ordinary and partial differential equations in science, finance, and engineering [10] and different advances has been contributing in the expanding field of algebraic topology. The homotopy method was applied in practical cases to solve nonlinear algebraic equations by Davidenko [11], around the 1960s in pure mathematics [12]. The idea behind the technique consists of transforming a particular complex system problem into a user-friendly problem. Behind this change in the system, the appropriate employment of parameters allows it to be gradually transformed from an initial operating point to an end point, namely, the solution of the original problem.

In general, the spectrum of applications for the homotopy theme is quite broad, even for just the power flow topic. Therefore, although the same can be investigated for a grid with different characteristics, the focus of this work is on the case in which the network is modeled only by the positive sequence network.

1.2 Study Motivation

The motivation of this study is to investigate the methods of load flow solutions and understand their advantages and drawback face of large scale power systems, simulating real scenarios. In normal operation, the system load changes in a predictable manner such that in the load flow study, the state of the previous scenario can be used as a starting point for the calculation of current flows. However, power systems are subject to contingencies that can displace the point of operation significantly [13]. Severe contingencies can take the operating point away from the starting point, which can hinder the work of the load flow solvers.

Knowing that conventional methods, such as Newton-Raphson method, are dependent on initial estimate and present local convergence, the initial estimate close to the solution of the problem is decisive to obtain the convergence in large scale systems, which can be difficult to obtain in the case of severe contingencies.

Therefore, it is intended to investigate a solver capable of solving the load flow problem starting from the flat start initialization, since it is a practical situation when the user have no other information on the operational equilibrium point of the system.

1.3 Objectives

The main objective of this work is to investigate the advantages of the homotopy method applied to the solution of the load flow problem considering the large-scale and ill-conditioned problems.

The specific objectives are:

- Presentation of a homotopy-based technique for determining the PFP solution based on the inclusion of an artificial admittance network.
- Development of the PFP solution technique with initial flat start estimation, regardless of network size.
- Proposition of a technique with two homotopy parameters, allowing better control of the homotopy process, aiming to depart from an initial estimates closer to the intermediate solutions that are calculated using the traditional NR method.
- Investigation of the impact due to the insertion of artificial strength interconnections with the slack bus, whose control is carried out by a scaling factor introduced as a function of a complementary homotopy process.

1.4 Contributions

The main contribution of the work lies in the method's ability to solve the power flow problem in large systems starting from a flat start guess, which is not possible from known solvers. In addition, the method proved to be versatile as it was able to successfully solve both well-conditioned and ill-conditioned systems. Another important point, through adjustments of input parameters in MATPOWER, any electrical system can be modeled and simulated in GSH-NR.

Considering the specific objectives, this work presents a homotopy-based method of calculating the solution to a power flow problem starting from a flat initial guess. Initial estimation of this nature attributed to a Newton-Raphson-based method for the PFP is desirable in the situation in which one does not have a history of operating point results of the network configuration under analysis, and when dealing with ill-conditioned systems. Mainly when carrying out studies in large-scale and practical networks. The idea is to exploit two physical aspects of the network and embed them into the homotopy process with the purpose of beginning all simulations from a flat start estimate. One aspect is related to the creation of an artificial local generation/load; a second aspect is related to the slack bus control to generate or absorb power along a typical homotopy process evolution. The methodology consists of structuring the PFP equations to incorporate a fictitious additional network with shunt admittances. The admittances in question are appropriately dimensioned so that the initial solution of the problem is exactly equal to the initial estimate (flat start). This physically means that an artificially local generation is created to supply its own load. Additionally, local generation can supply power to an artificial local load. With this aim, there is no angular difference between any two buses. These admittances are progressively overcome with the advancement of the homotopy process, which is controlled by a first homotopy parameter varying from a null to a unitary value. Thus, advancing by one step in the homotopy process, a portion of the shunt admittances created is removed. A second homotopy parameter and a scaling factor are used to strengthen interconnections close to the generation bus that is selected as the slack bus. This strengthening process is kept only along the intermediate homotopy process. When the first homotopy parameter reaches the unity value, the shunt admittance network is completely removed, and the scaling factor used in the second process is also removed. At this point in the process, the resulting network coincides with the original network, which is effectively the model used to determine the PFP final solution. The adopted strategy allows using the traditional NR method at each value of the first homotopy parameter. In this case, the result of the previous step is used as the estimate for the iteration in progress. Hence, an initial estimate for each NR application is always used at the boundary of the solution, providing convergence with a very small number of iterations, i.e., 2 to 4. Experiments considering several test systems, including a 70,000-bus system are used to demonstrate the effectiveness of the proposed methodology.

1.5 Related Publication

This research provided the following contributions:

- A. L. Silva and F. D. Freitas, "Investigation Study on the Voltage Stability Status of a Power Flow Problem Solution," 2021 Workshop on Communication Networks and Power Systems (WCNPS), 2021, pp. 1-6, doi: 10.1109/WCNPS53648.2021.9626316.
- F. D. Freitas and A. L. Silva, "Flat Start Guess Homotopy-based Power Flow Method guided by Fictitious Network Compensation Control" Submitted to the journal International Journal of Electrical Power and Energy Systems, 2022 (Article accepted).

1.6 Organization

In addition to this Chapter 1, this work is organized as fallows. It has the

- Chapter 2, where a bibliographic survey was carried out in order to identify research related to homotopy and recent power flow advance studies;
- Chapter 3, where the basic equations of the PFP are described and some techniques employed to solve power flow equations;
- Chapter 4, where the expressions to calculate the compensation admittances for the homotopy problem are presented. An initial flat start estimate and a flat start first homotopy (user-friendly) solution are also assumed, given that the compensation network composed of the fictitious admittances is fully connected;
- Chapter 5, which introduces the homotopy-based method proposed in this work, illustrating how the fictitious network is connected according to the homotopy process;
- Chapter 6, where several experiments and results are presented, to demonstrate the efficacy of the proposed homotopy-based technique;
- Conclusion, for concluding the work.

Chapter 2

Literature Review

2.1 Introduction

A bibliographic survey of scientific papers was done in scientific databases in order to verify the advances on the theme investigated in this work. The objective is to introduce the homotopy method, its main fields of application, the evolution of studies and the application in practical cases. To this end, it was proposed a systematic review of the main topics concerned to the Homotopy and Power Flow Problem.

2.1.1 The Power Flow Problem and Homotopy

Over the years, several references can be found in the application of homotopy methods. Recently, several techniques have been proposed, which use the homotopy method, by considering distinct approaches for solving the PFP. Chiang et al. [14] proposed to solve a power flow convergence problem found in some traditional power flow methods, when applied to distribution network with dispersed generations modeled as PV nodes. The use of homotopy methods improved a convergence property of the implicit Z-bus Gauss-Seidel method. In this work, the distributed generation was modeled initially as PQ bus, however being converted to PV bus in the last stage. The power flow solution was obtained by using homotopy method and considering a set of parameterized power flow equations. The proposed method was applied to IEEE 13-bus, IEEE 123-bus, IEEE 8500-node test system and a practical 1101-node distribution network. The systems was tested comparing implicit Z_{bus} method and homotopy-enhanced method with different homotopy steps. The evaluation of 3-stages methods has exhibited robust numerical properties and results were promising. However, this work did not give analytical results to explain the significantly improved convergence of the 3-stage method. To fill this gap, Chiang et al. [15] developed a new theory for general homotopy methods to show the convergence of the homotopy-enhanced implicit Z-bus PF method.

Pandey et al. [16] proposed a robustness method to solve the PFP of large-scale systems from arbitrary initial guesses. To achieve the correct physical solution, the network was modeled using equivalent circuit formulation. The modeling is based on true state variables of voltages and currents and uses circuit simulation methods to ensure robust convergence. Based on G-min stepping method [16], the transmission lines and transformer are virtually shorted, adding in parallel a large admittance for finding a trivial solution of the PFP. The homotopy method was used to determine incrementally subsequent solutions of a PFP sub-problem. Each sub-problem has a solution very close to the last one and the system is gradually be recomposed according to the increment of the homotopy parameter, until it reaches the original system topology. The method was tested at different ill-conditioned systems, as 11-bus system, 13659-bus system considering ten arbitrary initial conditions, and six distinct test systems, varying from 75k to 80k buses. The work shows that the homotopy continuation method with equivalent circuit achieves convergence to the correct physical solution and demonstrates robust convergence to the high voltage solution from an arbitrary initial guess.

Trying to overcome the weakness of ill-conditioned problem and poor initial start point conditions, typical of the standard Newton-Raphson method, Murray et al. [17] proposed techniques based on homotopy method to improve performance on large-scale power flow cases. Three different ways were proposed to improve the robustness of NR-based methods against poor initial points. One technique was called Injection Homotopy (IH). By this approach, virtual generators and loads are added to the network in such way that the power flow equations are solved with initial guess sufficiently close of each one. Following the same idea, a Phase Homotopy (PH) method was also proposed. The idea is to add virtually line phase shift to the network in such way that departing from an flat start initial guess the PFP is solved. The third approach was denominated Magnitude Homotopy (MH) method. It is based on points having near voltage magnitudes in relation to a reference, which make the region with physically meaningful attractive solutions. The approaches were tested for 1.2k-, 2.5k- and 46k-bus networks of two distinct North American Independent System Operators. However, just the last one method shows robustness for solving the cases with different starting points.

Yang et al. [18] used a homotopy and asymptotic numerical method for presenting a robust numerical method to solve the power flow equations. The asymptotic method, based on the computation of Taylor series expansion per step, provides an analytical continuous representation of the path to find solutions solving a simple polynomial equation. As well known that homotopy path often uses predictor-corrector path which has high computational cost, the asymptotic numerical method enhanced the efficiency of the homotopy continuation, mainly in ill-conditioned cases. At this study the generator reactive power limits was considered and the method uses flat start as initialization for voltage unknowns. The proposed method has been tested initially by using a 2-bus system. The NR method applied for this system converged slowly, with 17 iterations. However, the proposed method takes

only 6 steps with the same accuracy. Other systems has been tested, as 3-bus power systems, 43-bus ill-conditioned power system and 3375-bus power system considering the generator reactive power limits constraints. The numerical examples show improvements at computational steps and computational time compared with the Newton's method, and be reliable to solve the ill-conditioned power flow problems.

Jereminov et al. [19] proposed a homotopy-based method considering virtual changes in the network to solve the PFP. The problem is formulated by artificially creating shorted circuit in equipment. The method consists in using large conductance from each node to the ground. The grid parameters are changed, however the network topology is preserved at the final stage of the homotopy process. Applying a homotopy factor μ to change the network, the method suggest that the initial homotopy solution is more close to an intermediate solution than the original network solution. The process of computing this intermediate solution and using it as initialization for the next step improves convergence properties of the method. In order to simulate the real operate conditions the method has been tested in different large-scale systems, as 9241-, 10k-, 13659-, 25k-, and 70k-bus systems and other synthetic test cases. The tests show efficiency and robustness considering large-scale systems and ill-conditioned cases.

2.1.2 Optimal Power Flow

Optimal Power Flow (OPF) is an important tool for power system network analysis. The main objective of the OPF method is to find the lowest cost of producing electricity, considering the constraints of the elements that make up the network. With this objective, different scenario possibilities are presented in scientific papers aiming to test solvers in real power systems.

Park et al. [20], considering post-contingency scenarios, proposed to find a viable global solution for the large-scale OPF problem to assist system operators in preventive and corrective actions using homotopy methods. In this work the contingency, which is represented by equipment failure, was simulated only on line outages, setting the impedance of the line to a very high value. The contingency was introduced gradually with two homotopy parameters that allow to trace a gradual line outage event, instead an abrupt line outage event. The initial guess was provided by a standard case, without contingency. Testing different lines outages on Polish networks, with 3374-bus network, and varying the homotopy parameters, was ensured convergence to a global solution with better performance under certain conditions.

On the other hand, whereas the OPF try to find the global optimum for the problem, find a local convergency can be a challenging. In this regard, Pandey et al. [21] proposed a robust local convergence with homotopy-based approach that solves a sequence of primal-dual interior point problems for large systems as U.S. Eastern Interconnection sized test networks

Zárate-Miñano et al. [22] proposed a practical application for OPF considering different load models. The loads considered were the maximum number of plug-in electric vehicles that were inserted into the power system using homotopy-method to measure quantitatively and qualitatively. Four models, which differ in the way electric vehicles are integrated into the network, were simulated in the IEEE One Area RTS-96 with 24-bus system. The homotopy factor represented the number of vehicles inserted in the network. From a quantitative point of view, the choice of model shows a significant difference in the number of vehicles inserted in the system and in the quality of the loading of the system buses.

Molzahn et al. [23] proposed a algorithm that compute all OPF feasible spaces by discretizing OPF problem's inequality constrains to get a set of power flow equations. Same inequalities of OPF problem is discretized into equality constrains and the numerical polynomial homotopy continuation was used to compute all solutions at each discretization point. The method was tested for two small OPF problems, 5- and 9-bus systems, due to the intractability of numerical polynomial homotopy continuation for large problems. The algorithm uses continuation to trace all the complex solution from start system, with trivially solution, to a original system along one-dimensional parameter.

2.1.3 Integration of Renewable Energies

With the popularization of the production of energy from renewable sources, the modeling of the electric power system has become a challenge. This is justified since renewable energy sources are intermittent, such as wind and solar energy, and they are typically accompanied by the presence of energy storage elements. In this sense, power flow studies have incorporated these new technologies into various areas of knowledge. Tests have been carried out on large systems and their robustness is tested in several aspects to verify the impact of the large-scale integration of renewable energies and new types of loads.

Agarwal et al. [24] proposed a multi-period optimal power flow as a large non-convex nonlinear problem to optimally dispatch and control generators and energy storage elements. The problem considers multiple time periods using a scalable and robust framework to solve the problem using a differential dynamic programming scheme that consider energy storage devices. Using the state at previous time, multi-period optimization was modeled for energy storage and generator ramping are inherently time-variant. The energy storage system was modeled charging and discharging power into the grid. The homotopy methods was used to determine the state vector using the factor γ_{NS} varying 1 to 0 for changing power and switching on or off conductances and susceptances, using the period's time solution as an initial condition and iteratively solves sub-problems leading to the optimal dispatch. The framework was tested with the small system IEEE-14 bus, modified to include the energy storage system, and large system like 70k+ bus SyntheticUSA initialized by flat start, 1 pu voltage magnitude and 0 voltage angle, to demonstrate efficiency and scalability. The algorithm allow further speedup and the framework offers a robust tool to study OPF and

exploring a large-scale optimization studies.

Chandra et al. [25] used different types of energy generators and elements to simulate the impact of large-scale integration, as renewable, storage elements and dynamic loads. The results was illustrated though the simulation of a 5-machine power system model with wind, storage elements, and dynamic loads, into 7-bus system. In that work, they considered battery energy system in the wind power plant together with dynamic loads. Considering that this systems has different parameters, they used homotopy methods to compute equilibrium points using differential-algebraic model of the power system, parameterized by elements, considering the nonlinear swing dynamics, wind power dynamics, battery model, load dynamics and power flow. The solution set consists of a finite number of smooth paths parameterized by homotopy factor that find an isolated solution using an predictor-corrector method to find all the paths. The results show the entire parameter space using the homotopy based algorithm solve efficiently the set of equations, and was used to evaluate all the equilibria in an efficient manner.

Bie et al. proposed studies based on online multi-period power dispatch with AC constraints and renewable energy [26] and with renewable uncertainty and storage [27] for solving OPF. Using the AC power flow equations, voltage limits, and thermal limits the solution is ensured with no static violation and guaranteeing transfer capability. The renewable energy sources are incorporated into the problem formulation using scenario generation tool to generate renewable scenarios. The formulation takes into account linear and nonlinear dependence between different renewable energy sources generated from historical data. A four- and three-stage solution methodology was proposed to solve the problem using an adaptive homotopy-enhanced primal-dual interior point method and two-parameters homotopy-enhanced method. Whereas the problem is solved in stages the method the homotopy methodology was applied at first- and third-stage in [27], and fourth stage in [26]. The solutions was evaluated on IEEE 30-, IEEE 118-, IEEE 300- and 3012-bus system and presented robustness and efficiency.

2.1.4 Voltage Stability

A power system is defined as robustness when operate in a state of equilibrium in normal condition or some disturbance of parameters [4]. However, there are a lot of phenomena that can cause network instability. For instance, events that change the transmission line parameters can lead a system to voltage instability [28]. Hence, understanding of the stability phenomena is a challenging for the voltage stability analysis considering it as a common instrument for monitoring the network power flow by operators. Contingencies in the system can be fast, in the order of seconds, or even longer with minutes. Therefore, understanding interference, and finding ways to simulate them and predict scenarios, is of great value for preventive and corrective actions.

Many recent studies have treated the subject based on homotopy techniques to solve the

problem. Burgos et al. [29] proposed to combine homotopy techniques with quasi-steady-state methods that consider both, static and dynamic aspects of the power system, to analyze voltage stability efficiently from the point of view of the load margin. The idea is to use the continuation factor associated with the time variable and the load variation to estimate the saddle node bifurcation. The method was tested in the BOL 162-bus system and proved to be suitable to calculate the load margin of a power system from the point of view of voltage stability.

Using a scenario with large insertion of distributed generation, that may result in the reversal power flow, Nguyen et al. [30] demonstrated the multistability phenomenon in radial distribution and did a voltage stability analysis introducing admittance homotopy power flow method to find solutions. The results was validated with dynamic simulations on IEEE 13-bus and the method has better results than other traditional methods.

Kettner et al. [31] studied the impact of Kron reduction into numerical methods applied to the analysis in unbalanced polyphase power systems. Among them, homotopy continuation method was tested for voltage stability assessment. The main performance indicators of this method are the number of steps to the solution and the computation burden. Results of the Kron reduction showed that the steps fell by half and the running time decreased by a factor of 10 and confirm the applicability of Kron reduction for this analysis.

2.2 Conclusion of this chapter

In this chapter, a bibliographic revision was carried out in scientific databases to identify recent studies on the themes power flow and homotopy. It can be stated that the concepts of homotopy are associated with solutions to the power flow problem with distinct robust approaches applied to large-scale cases starting from arbitrary points and for ill-conditioned cases. Themes as optimal power flow, integration of intermittent renewable energy sources, voltage stability were found and also motivated the present work.

In addition, the works related to the theme of this work appear in recent papers dating from 2016 to 2020, which demonstrates the relevance of the proposed research.

Chapter 3

The Power Flow Problem Formulation

3.1 Introduction

A classical problem of electric circuit theory is to model the system by the impedance between branches as well as the voltage parameters of the generators, to result in the calculation of current flow and voltages in the nodes. The solution of the equation of these characteristics involves the solution of algebraic equations because the interest is the determination of an operation point [7].

However, there is a key difference in the input data of the system that governs the mathematical approach to treat the problem. The system loads are modeled as active and reactive power, constant power consumption, resulting in set of nonlinear equations. Therefore, the aggregation of this information generates a set of nonlinear equations that is normally solved numerically.

Thus, in order to solve nonlinear problems by numerical methods, many researchers proposed solutions with advantages and drawbacks from different points of view. The ones that will be shown in this chapter are directly linked to applications in the load flow and are well known in the literature.

3.2 The Power Flow Problem

An energy transmission system is basically composed of elements such as interconnections, device models, load, generations, and other characteristics with device ceilings, transformer tap control, capacitor/reactor switching, etc. This set of elements compose the network parameters and can be modeled in order to form the network equations [4]. The Kirchhoff law relating current and voltage on each bus can be put as:

$$\begin{bmatrix} \overline{I}_1 \\ \overline{I}_2 \\ \vdots \\ \overline{I}_n \end{bmatrix} = \begin{bmatrix} Y_{11} & Y_{12} & \cdots & Y_{1n} \\ Y_{21} & Y_{22} & \cdots & Y_{2n} \\ \vdots & \vdots & \ddots & \vdots \\ Y_{m1} & Y_{m2} & \cdots & Y_{mn} \end{bmatrix} \cdot \begin{bmatrix} \overline{V}_1 \\ \overline{V}_2 \\ \vdots \\ \overline{V}_n \end{bmatrix} \Leftrightarrow \left[\overline{I}\right] = \left[Y_{bus}\right] \cdot \left[\overline{V}\right] \tag{3.1}$$

where:

$\overline{I}_n$	phasor current injected into the network at node n;
$\overline{V}_n$	phasor voltage to ground at node n;
Y_{ii}	self admittance of the matrix $[Y_{bus}]$ in the node i;
Y_{ij}	mutual admittance of the matrix $[Y_{bus}]$ between nodes i and j;
n	number of nodes;
$\left[\overline{I}\right]$	injected current vector;
$\left[\overline{V}\right]$	nodal voltage vector;
$[Y_{bus}]$	admittance matrix.

Therefore, the current in the k^{th} node is given by (3.2):

$$\overline{I}_k = \sum_{m=1}^{N_b} \overline{Y}_{km} \overline{V}_m. \tag{3.2}$$

The complex power is defined as [32]

$$\overline{S}_k \ = \ P_k \ + jQ_k = \overline{V}_k \overline{I}_k^* \tag{3.3}$$

$$P_k \ + jQ_k = \overline{V}_k \left[\sum_{m=1}^{N_b} \overline{Y}_{km} \overline{V}_m \right]^* . \tag{3.4}$$

Moreover, $\overline{V}_k = V_k e^{j\theta_k}$, $\overline{V}_m^* = V_m e^{-j\theta_m}$ and $\overline{Y}_{km}^* = G_{km} - jB_{km}$. Then, replacing it in (3.4)

$$P_k \ + jQ_k = V_k \sum_{m=1}^{N_b} (G_{km} - jB_{km}) V_m e^{j(\theta_k - \theta_m)}. \tag{3.5}$$

The angular difference between bus k and m is $\theta_k - \theta_m = \theta_{km}$. Using Euler's formula, where $e^{j\theta_{km}} = \cos\theta_{km} + j\sin\theta_{km}$, it is obtained

$$P_k \ + jQ_k = V_k \sum_{m=1}^{N_b} V_m (G_{km} - jB_{km}) \left[\cos(\theta_{km}) + j\sin(\theta_{km})\right]. \tag{3.6}$$

Finally, by reorganizing (3.6) and separating the imaginary from the real part, the net active power injected into bus $\#k$, P_k, and the net reactive power injected into the same bus, Q_k,

are

$$P_k = V_k \sum_{m=1}^{N_b} V_m \left[G_{km} \cos(\theta_{km}) + B_{km} \sin(\theta_{km}) \right] \qquad k = 1, 2, \ldots, N_b \tag{3.7}$$

$$Q_k = V_k \sum_{m=1}^{N_b} V_m \left[G_{km} \sin(\theta_{km}) - B_{km} \cos(\theta_{km}) \right] \qquad k = 1, 2, \ldots, N_b. \tag{3.8}$$

The injected power $\overline{S}_k$ can be composed of a load demand $\overline{S}_{Dk}$ plus a power generated $\overline{S}_{Gk}$ in the bus k, resulting in the net power P_k and Q_k

$$\overline{S}_k = \overline{S}_{Gk} - \overline{S}_{Dk} \begin{cases} \overline{P}_k = \overline{P}_{Gk} - \overline{P}_{Dk} \\ \\ \overline{Q}_k = \overline{Q}_{Gk} - \overline{Q}_{Dk}. \end{cases} \tag{3.9}$$

By considering (3.7) and (3.8), there are four variables V_k, θ_k, P_k and Q_k associated to each bus. Depending on the type of bus, two of them need to be specified and the other ones must be calculated. These buses can be categorized as three types [32]. A first type called slack bus, named also swing bus. It is used as reference bus, where voltage magnitude and the voltage angle are given and are used to balance the system losses. A second type denominated PQ bus, also named as load bus, where active and reactive power are specified. In this bus the voltage magnitude and phase angle are computed. Usually, it represents the bus where a load is connected. Finally, the PV bus, named also as controlled voltage bus, where a voltage source is connected. In this bus the voltage phase and reactive power are calculated. Usually in the PV buses, reactive power constraining must be taken into account [33]. Tab. 3.1 summarizes the buses type with input and computed data.

Table 3.1: Buses type

Bus Type	Named as	Input data	Computed data
Slack bus	Swing bus	$V_k \quad \theta_k$	$P_k \quad Q_k$
PQ bus	Load bus	$P_k \quad Q_k$	$V_k \quad \theta_k$
PV bus	Controlled voltage bus	$P_k \quad V_k$	$Q_k \quad \theta_k$

The power flow problem (PFP) for a network of N_b buses consists of solving a nonlinear system of algebraic equations, (3.7) and (3.8), representing the system modeled before excluding the slack bus equations. This exclusion is justified since the states associated to the slack bus are known (bus voltage magnitude and angle). Also, for the polar representation of voltages, the equations related to the reactive power balance equations can be removed from (3.8). Mathematically, this set of information leads to the classical power balance equations (PBEs). The general set of nonlinear equations for a generic bus $\#k$ for PQ- and PV-type

will be given by the standard net power injection formulation in polar form:

$$0 = P_k - V_k \sum_{m=1}^{N_b} V_m \left[G_{km} cos(\theta_{km}) + B_{km} sin(\theta_{km}) \right], \;\; k \in PQ \; or \; PV \tag{3.10}$$

$$0 = Q_k - V_k \sum_{m=1}^{N_b} V_m \left[G_{km} sin(\theta_{km}) - B_{km} cos(\theta_{km}) \right], \;\; k \in PQ. \tag{3.11}$$

Assume that the set of PQ buses will be denoted by N_{PQ}; the set of PVs, by N_{PV}; and the AC network is synchronous with only one slack bus in such way that $N_b = N_{PQ} + N_{PV} + 1$. For convenience, bus $\#1$ is *labeled as the slack bus* in this work, and the voltage at this bus has a known real value, V_0. Hence, the number of equations (3.10)-(3.11) is $n = 2N_{PQ} + N_{PV}$. Then, a compact notation for the set of nonlinear equations is given by

$$\mathbf{f}(\mathbf{x}) = \mathbf{0} \tag{3.12}$$

where $\mathbf{x} = \left[\boldsymbol{\theta}^T \; \boldsymbol{V}^T \right]^T \in \mathbb{R}^n$ is the network state and $\mathbf{f}(\mathbf{x})$ is a map of the type $\mathbf{f}(\mathbf{x}) : \mathbb{R}^n \mapsto \mathbb{R}^n$.

In general, the PBE solution is determined numerically using iterative methods. In the sequence, we describe how this process can be carried out by exploring some numerical techniques.

3.2.1 Gauss-Seidel method

The Gauss-Seidel method is an iterative method that estimates the bus voltage from the active and reactive power delivered by the generation or supplied to the load connected, the estimated voltages in the adjacent buses and the impedance associated with that bus [34]. As an implicit method, when the solution at x_{n+1} use data from previous point x_n and an initial estimate at point x_{n+1}, like a corrector algorithm, in each iteration an new set of voltages are obtained and solutions are approaching the response until a maximum error is reached. Starting by power equation (3.3), the current can given by (3.13) or expressed by admittance and voltage associated (3.15)

$$\overline{I}_k = \frac{P_k - jQ_k}{\overline{V}_k^*} \tag{3.13}$$

$$\frac{P_k - jQ_k}{\overline{V}_k^*} = \overline{Y}_{kk}\overline{V}_k + \sum_{\substack{n=1 \\ n \neq k}}^{N_b} \overline{Y}_{kn}\overline{V}_n. \tag{3.14}$$

The voltage at PQ-bus k is given by

$$\overline{V}_k = \frac{1}{\overline{Y}_{kk}} \left[\frac{P_k - jQ_k}{\overline{V}_k^*} - \sum_{\substack{n=1 \\ n \neq k}}^{N_b} \overline{Y}_{kn} \overline{V}_n \right]. \tag{3.15}$$

For PV-bus the reactive power shall be calculated first using equation (3.16)

$$P_k - jQ_k = \left(\overline{Y}_{kk} \overline{V}_k + \sum_{\substack{n=1 \\ n \neq k}}^{N_b} \overline{Y}_{kn} \overline{V}_n \right) \overline{V}_k^* \quad \text{with } n = k, \text{ then} \quad P_k - jQ_k = \overline{V}_k^* \sum_{n=1}^{N_b} \overline{Y}_{kn} \overline{V}_n$$

$$Q_k = -Im \left(\overline{V}_k^* \sum_{n=1}^{N_b} \overline{Y}_{kn} \overline{V}_n \right) \tag{3.16}$$

and then, by applying the result in the equation (3.15). The method solves one equation at a time and uses the values obtained in subsequent iterations.

3.2.2 Newton-Raphson method

A standard technique employed to solve power flow equations is the Newton-Raphson iteration method. Whereas the power flow equations, $\mathbf{f}(\mathbf{x})$, are formed by nonlinear algebraic equations, the intention is to determine the value of $\mathbf{x}$ for which the function $\mathbf{f}(\mathbf{x}) = 0$. Considering an initial estimate $\mathbf{x}^{(0)}$ near the solution of problem $\mathbf{x}_*$, one can determine the distance between $\mathbf{x}^{(0)}$ and $\mathbf{x}_*$ by expanding the function $\mathbf{f}(\mathbf{x})$ close to $\mathbf{x}^{(0)}$.

Let $\mathbf{f}(\mathbf{x}) \in \mathbb{R}$ be a scalar function where $\mathbf{x} \in \mathbb{R}$. The expansion of $\mathbf{f}(\mathbf{x})$ in Taylor series around estimate $\mathbf{x}^{(0)}$ is given by

$$\mathbf{f}(\mathbf{x}) = \sum_{n=0} \frac{\mathbf{f}^{(n)}\left(\mathbf{x}^{(0)}\right)}{n!} \left(\mathbf{x} - \mathbf{x}^{(0)}\right)^n$$

$$\mathbf{f}(\mathbf{x}) = \mathbf{f}\left(\mathbf{x}^{(0)}\right) + \mathbf{f}'\left(\mathbf{x}^{(0)}\right)\left(\mathbf{x} - \mathbf{x}^{(0)}\right) + \frac{\mathbf{f}''\left(\mathbf{x}^{(0)}\right)}{2!}\left(\mathbf{x} - \mathbf{x}^{(0)}\right)^2 + \frac{\mathbf{f}'''\left(\mathbf{x}^{(0)}\right)}{3!}\left(\mathbf{x} - \mathbf{x}^{(0)}\right)^3 + \cdots$$

A linear approximation, i.e., disregarding higher order terms greater than one, yields

$$\mathbf{f}(\mathbf{x}) \approx \mathbf{f}\left(\mathbf{x}^{(0)}\right) + \mathbf{f}'\left(\mathbf{x}^{(0)}\right)\left(\mathbf{x} - \mathbf{x}^{(0)}\right). \tag{3.17}$$

Given that $\mathbf{f}(\mathbf{x}) = 0$, then

$$\mathbf{x} - \mathbf{x}^{(0)} = -\frac{\mathbf{f}\left(\mathbf{x}^{(0)}\right)}{\mathbf{f}'\left(\mathbf{x}^{(0)}\right)}$$

with $\mathbf{x} - \mathbf{x}^{(0)} = \Delta\mathbf{x}$, then an linear approximation of $\mathbf{f}(\mathbf{x})$ around $\mathbf{x}^{(0)}$ is

$$\mathbf{f}(\mathbf{x}) \approx \mathbf{f}\left(\mathbf{x}^{(0)} + \Delta\mathbf{x}\right) \approx \mathbf{f}\left(\mathbf{x}^{(0)}\right) + \left[\left.\frac{\partial \mathbf{f}}{\partial \mathbf{x}}\right|_{\mathbf{x}^{(0)}}\right] \Delta\mathbf{x} \approx 0. \tag{3.18}$$

The iterative solution of the NR method for the ith iteration is obtained as

$$\mathbf{x}^{(i+1)} = \mathbf{x}^{(i)} + \Delta\mathbf{x}^{(i)} \tag{3.19}$$

where the increment $\Delta\mathbf{x}^{(i)}$ is computed for a mismatch $\mathbf{f}(\mathbf{x}^{(i)})$ as

$$\Delta\mathbf{x}^{(i)} = -\left[\mathbf{J}\left(\mathbf{x}^{(i)}\right)\right]^{-1} \mathbf{f}(\mathbf{x}^{(i)}) \tag{3.20}$$

and Jacobian matrix for $\mathbf{f}(\mathbf{x}) \in \mathbb{R}^n$ and $\mathbf{x} \in \mathbb{R}^n$ as

$$\mathbf{J}(\mathbf{x}^{(i)}) = \left.\frac{\partial \mathbf{f}(\mathbf{x})}{\partial \mathbf{x}}\right|_{\mathbf{x}^{(i)}} = \begin{bmatrix} \frac{\partial \mathbf{f}_1(\mathbf{x})}{\partial \mathbf{x}_1} & \frac{\partial \mathbf{f}_1(\mathbf{x})}{\partial \mathbf{x}_2} & \cdots & \frac{\partial \mathbf{f}_1(\mathbf{x})}{\partial \mathbf{x}_n} \\ \frac{\partial \mathbf{f}_2(\mathbf{x})}{\partial \mathbf{x}_1} & \frac{\partial \mathbf{f}_2(\mathbf{x})}{\partial \mathbf{x}_2} & \cdots & \frac{\partial \mathbf{f}_2(\mathbf{x})}{\partial \mathbf{x}_n} \\ \vdots & \vdots & \ddots & \vdots \\ \frac{\partial \mathbf{f}_n(\mathbf{x})}{\partial \mathbf{x}_1} & \frac{\partial \mathbf{f}_n(\mathbf{x})}{\partial \mathbf{x}_2} & \cdots & \frac{\partial \mathbf{f}_n(\mathbf{x})}{\partial \mathbf{x}_n} \end{bmatrix}.$$

The iterative value $\mathbf{x}^{(i+1)}$ converges numerically to the root $\mathbf{x}_*$ when $\|\mathbf{f}(\mathbf{x}_*)\|_\infty < \epsilon$ for $\epsilon > 0$ is sufficiently small, where

$$\|\mathbf{f}(\mathbf{x}_*)\|_\infty = max\left\{|f_1|, \ldots, |f_n|\right\}.$$

In case the convergence is not verified for a specified number of iterations, say max_{iter}, we consider that the problem is divergent and the iterative process is interrupted.

The classical methods employed to solve the power flow problem consider the Gauss-Seidel (GS), Newton-Raphson (NR) methods and their variants which are based on simplifications carried out in the Jacobian matrix. Techniques such as the Fast Decoupled (FD) among others ones are some examples. The NR method is the standard method used in industrial applications [8]. However, the performance of a power flow method is strongly dependent of the system condition mainly due to the following factors [35]:

i. Large number of radial lines.

ii. Heavy loading conditions.

iii. Existence of negative line reactance.

iv. Lines with high resistance to reactance ratios.

v. Initial guess point outside of the region of attraction or far away from the solution.

The aforementioned characteristics can cause divergence for most standard PFP solver methods based on NR. In this case, the system is said as ill-conditioned [7, 8]. The solution of a power flow for ill-conditioned cases is still a challenging even for most of the available robust methodologies [35].

Milano in [8] classifies the PFP into four categories as follows: 1) well-conditioned, when the PF solution exists and is reachable using a flat initial guess (i.e., all load voltage magnitudes equal to 1 and all bus voltage angles equal to 0) and a standard Newton–Raphson's method; 2) ill-conditioned, when the solution of the PFP does exist, but standard solution methods fail to get this solution starting from a flat initial guess; 3) bifurcation point, whose solution of the PF exists but it is either a saddle-node bifurcation or a limit-induced bifurcation; and 4) unsolvable, when the PF solution does not exist.

There is a situation where the initial guess is inside the region of attraction of the solution point. Then, in this case, the NR method applied to this situation is expected to converge. However, in some cases, it can occur divergence. In this case the initial guess is far away from the solution and robust numerical methods should be used before the NR method.

A commonly used situation when solving the PFP is starting from an estimate of the type *flat start*. However, when dealing with large systems, this alternative may fail when using the traditional NR method. Several robust methods have been developed in order to solve the ill-conditioned cases associated with the PFP solution. A technique based on the Newton-Continuous philosophy were proposed in [8].

3.3 The Newton's Continuous Philosophy

For better understanding, the introduction of the Newton-Continuous method, it is explained, initially, based on an analogy with the representation of a non-linear continuous dynamical system in the time domain. And then, on its analog simulation in the time domain using a numerical integration method.

Assume that (3.21) represents the standard form for the notation of a set of ordinary differential equations (ODEs) of an autonomous system.

$$\dot{\mathbf{x}}(t) = \mathbf{g}(\mathbf{x}(t)) \tag{3.21}$$

where $\mathbf{x}(t) \in \mathbb{R}^n$, $\mathbf{g}(\mathbf{x}(t)) \in \mathbb{R}^n$ is a nonlinear function of $\mathbf{x}(t)$ and $\dot{\mathbf{x}}(t)$ represents the derivative with respect to a continuous parameter $t \in \mathbb{R}^+$. From the next paragraph, the

parameter t will be omitted from the argument of the variable $\mathbf{x}(t)$.

Equation (3.21) can be solved for the discrete time parameter t by a numerical integration method. The simplest method known in the literature is the explicit Euler, also known as forward Euler (FE) method, whose k-th step is performed as follows:

$$\begin{aligned} \Delta\mathbf{x}^{(k)} &= \Delta t\mathbf{g}\left(\mathbf{x}^{(k)}\right) \\ \mathbf{x}^{(k+1)} &= \mathbf{x}^{(k)} + \Delta\mathbf{x}^{(k)} = \mathbf{x}^{(k)} + \Delta t\mathbf{g}\left(\mathbf{x}^{(k)}\right) \end{aligned} \tag{3.22}$$

where Δt is the integration step, assuming that the variable $\mathbf{x}$ is a function of the parameter t; $\mathbf{x}^{(k)}$ is the vector with the values of $\mathbf{x}$ in step k; and $\Delta\mathbf{x}^{(k)}$ is the increment calculated in step k to obtain the result in step $k+1$ of the variable $\mathbf{x}$.

According to [8], assuming a nonsingular Jacobian matrix $\mathbf{J}(\mathbf{x})$ as defined for (3.20), a direct analogy between (3.20) and (3.22) allows one to write

$$\mathbf{g}\left(\mathbf{x}^{(k)}\right) = -\left[\mathbf{J}\left(\mathbf{x}^{(k)}\right)\right]^{-1}\mathbf{f}\left(\mathbf{x}^{(k)}\right). \tag{3.23}$$

Based on this analogy, the traditional NR method for solving nonlinear equations can be interpreted as an application of the explicit Euler method (see (3.22) with $\Delta t = 1$ to solve ODEs. From then on, the methodology became known as Newton's continuous method and began to be extended to other numerical integration approaches, in addition to the explicit Euler approach.

In the same work, Milano [8] proposed to use a Runge-Kutta approach to perform the numerical integration in (3.21) instead of the explicit Euler solver.

3.3.1 Runge-Kutta method

A classical fourth order Runge-Kutta method (RK4) was used to determine the PFP solution through the numerical integration of (3.21). The RK4 is an explicit numerical integration method based on computations of the state $\mathbf{x}_{n+1}$ from an solution at point $\mathbf{x}_n$. Considering a ill-conditioned system this method presents a better results compared to NR. The RK4 method is given by considering the following parts for composing the main computations at the i-th iteration [8]:

$$K_1 = \mathbf{g}\left(\mathbf{x}^{(i)}\right)$$

$$K_2 = \mathbf{g}\left(\mathbf{x}^{(i)} + 0.5\Delta tK_1\right)$$

$$K_3 = \mathbf{g}\left(\mathbf{x}^{(i)} + 0.5\Delta tK_2\right)$$

$$K_4 = \mathbf{g}\left(\mathbf{x}^{(i)} + \Delta tK_3\right)$$

$$\mathbf{x}^{(i+1)} = \mathbf{x}^{(i)} + \frac{\Delta t(K_1 + 2K_2 + 2K_3 + K_4)}{6}. \tag{3.24}$$

The mismatch can be estimated using the half-step of the equation (3.25).

$$\xi = max\left\{abs\left(K_2 - \mathbf{x}^{(i+1)}\right)\right\}. \tag{3.25}$$

The time interval Δt can be adapted based on the truncation error estimated in the integration method. Thus, the Δt step is adjusted according to the equation (3.26). Based on these rules, the time interval is increased if the truncation error is greater than a certain limit and decreased if the error is lower [8]. Then, the following rule is suggested for modifying Δt

$$\text{If } \xi > 0.01, \text{ then } \Delta t \leftarrow max\{0.985 \cdot \Delta t, 0.75\}$$

$$\text{If } \xi \leq 0.01, \text{ then } \Delta t \leftarrow min\{1.015 \cdot \Delta t, 0.75\}. \tag{3.26}$$

Aiming at an improvement of the Euler method proposed previously, Milano in [7] proposed to use the implicit (backward) Euler method, instead of the explicit one.

3.3.2 Backward Euler method

The application of the Backward Euler (BE) method involves some additional manipulations of the expression (3.21).

Considering the implicit differential equation, the equation (3.23) can be rewritten as (3.27) and be integrated by using a BE method [36]

$$\mathbf{J}\left(\mathbf{x}^{(k)}\right)\mathbf{g}\left(\mathbf{x}^{(k)}\right) = -\mathbf{f}\left(\mathbf{x}^{(k)}\right). \tag{3.27}$$

Now, we need to solve the set of nonlinear equation [36]

$$0 = \phi\left(\mathbf{x}^{(k)}\right) = \mathbf{J}\left(\mathbf{x}^{(k)}\right)\left(\mathbf{x}^{(k)} - \mathbf{x}^{(k-1)}\right) + \Delta t\mathbf{f}\left(\mathbf{x}^{(k)}\right). \tag{3.28}$$

The equation (3.28) can be solved by the Newton method, where the sub-index i in (3.29) (internal loop) indicates the i^{th} Newton iteration for the computation of the k-th step (external loop), given that the $k-1)-th$ step is known

$$\mathbf{x}_{i+1}^{(k)} = \mathbf{x}_i^{(k)} - \left[\phi_{\mathbf{x}}\left(\mathbf{x}_i^{(k)}\right)\right]^{-1}\phi\left(\mathbf{x}_i^{(k)}\right) \tag{3.29}$$

and $\phi_{\mathbf{x}}$ denote the Jacobian matrix for the function $\phi(\mathbf{x})$ and

$$\phi\left(\mathbf{x}_i^{(k)}\right) = \mathbf{J}\left(\mathbf{x}_i^{(k)}\right)\left(\mathbf{x}_i^{(k)} - \mathbf{x}^{(k-1)}\right) + \Delta t \mathbf{f}\left(\mathbf{x}_i^{(k)}\right). \tag{3.30}$$

To integrate this system we need to solve two loops, the inner over i and the main loop over k. To compute the term $\phi_{\mathbf{x}}^{(k)}$, it is needed to calculate the Hessian matrix of the power flow $\mathbf{H} = \mathbf{f}_{\mathbf{xx}}$ from (3.30), yielding

$$\phi_{\mathbf{x}}\left(\mathbf{x}_i^{(k)}\right) = \mathbf{H}\left(\mathbf{x}_i^{(k)}\right)\left(\mathbf{x}_i^{(k)} - \mathbf{x}_i^{(k-1)}\right) + (1 + \Delta t)\mathbf{J}\left(\mathbf{x}_i^{(k)}\right). \tag{3.31}$$

In view of the complexity for determining and implementing $\mathbf{H}$ for the case of the power flow in large-scale models, empirical tests were proposed and validated in [36]. Results of experiments have demonstrated that the term $\mathbf{H}(\mathbf{x}_i^{(k)})(\mathbf{x}_i^{(k)} - \mathbf{x}_i^{(k-1)})$ has little impact on the convergence process. Hence, the expression (3.31) can be drastically simplified when we consider $\mathbf{x}_1^{(k)} = \mathbf{x}_1^{(k-1)}$. Then, a reasonable approximation for (3.31) is

$$\phi_{\mathbf{x}}\left(\mathbf{x}_i^{(k)}\right) \approx (1 + \Delta t)\mathbf{J}\left(\mathbf{x}_i^{(k)}\right). \tag{3.32}$$

Therefore, (3.29) can be rewritten as follows

$$\mathbf{x}_{i+1}^{(k)} \approx \mathbf{x}_i^{(k)} - \left[(1 + \Delta t)\,\mathbf{J}\left(\mathbf{x}_i^{(k)}\right)\right]^{-1} \phi\left(\mathbf{x}_i^{(k)}\right). \tag{3.33}$$

Hence, with expressions (3.30) and (3.33), we find

$$\mathbf{x}_{i+1}^{(k)} \approx \mathbf{x}_i^{(k)} - (1 + \Delta t)^{-1}\left[(\mathbf{x}_i^{(k)} - \mathbf{x}^{(k-1)}) + \Delta t\left[\mathbf{J}\left(\mathbf{x}_i^{(k)}\right)\right]^{-1}\mathbf{f}\left(\mathbf{x}_i^{(k)}\right)\right] \tag{3.34}$$

which can be rewritten as

$$\mathbf{x}_{i+1}^{(k)} \approx \frac{1}{1 + \Delta t}\left\{\mathbf{x}^{(k-1)} + \Delta t\left[\mathbf{x}_i^{(k)} - \left[\mathbf{J}\left(\mathbf{x}_i^{(k)}\right)\right]^{-1}\mathbf{f}\left(\mathbf{x}_i^{(k)}\right)\right]\right\}. \tag{3.35}$$

We considered in this work an implicit continuous Newton method (ICNM) using BE with some simplifications, as proposed in [36] according to expression (3.35). In this solver, the Hessian matrix is neglected and the solution of the inner loop for the index i is approximated with its first iteration. The author in [36] labeled it as ICNM-J_1.

3.4 Conclusion of this chapter

This chapter presented the formulation regarding the power flow problem and some methods to solve the problem of an iterative form. The standard Gauss-Seidel method was introduced considering its historical employment in the past. The classical Newton-Raphson method was presented as a key tool for solving the PFP. However, its characteristics of local convergence gave space recently to several researches in order to search new and robust techniques to expand the convergence region of the PFP. In this sense, methods based on the Newton's continuous philosophy were proposed in the literature and reviewed in this work. Among them, techniques based on numerical integration for solving a problem represented by ODEs were discussed. Therefore, solver for nonlinear equations considering the Euler method (forward and backward) and Runge-Kutta were studied to be compared with other approaches involving the standard NR method.

In the next chapters a technique based on homotopy and using the NR method is proposed in order to solve ill-conditioned PFP.

Chapter 4

Fictitious Network Compensation

4.1 Introduction

It is well known that the NR method has quadratic convergence, and it is expected that it converges when an estimate $\mathbf{x}_0$ is in the solution attraction region. However, even for small equation systems, this estimate may be difficult to assign inside this region. Even taking place within this region, the iterative process can still diverge [7]. Additionally, practical results occur for a range of voltage magnitudes near network nominal voltages. In this sense, for the solution $\mathbf{x}_*$, the investigation in this work addresses the problem of finding a robust strategy to solve the PFP when $\mathbf{x}_*$ exists and the Jacobian matrix of $\mathbf{f}(\mathbf{x}_*)$ is nonsingular.

In this work, the objective is to *solve the nonlinear equations by an iterative method, departing from an estimate* $\mathbf{x}^{(0)}$ *equal to the flat start point*. Additionally, other strategies of initial estimate are investigated as Gauss-Seidel iterations and the DC Power Flow (DCPF) [37]. However, in this chapter only the initialization by assuming a flat start guess is addressed. This strategy ends up being recommended for cases where the user has no idea of the operating point of the system, such as when a previous operational condition is unknown, or even under conditions of severe contingencies. Therefore, starting from a nominal operating point always becomes a more conservative alternative.

The flat start initialization procedure which will be used further for the homotopy process is based on an inclusion of a fictitious network compensation according to the idea proposed in this work. Then, the objective in this chapter is to show how to form this fictitious network compensation, before introducing the homotopy process itself. This first stage is known as the "easy" solution at a process of homotopy. The procedure consists in determining an initial fictitious network that at the end of the homotpy solver is extinguished. This way, the state solution coincides with that one of the original power system model, i.e., without the compensation network.

4.2 Setting of a fictitious network compensation

The main purpose of this section is to explain the creation of a fictitious network for giving a PFP solution which is equal to the own initial estimate. With this aim, we intend to prepare the initial condition to formulate in the next chapter a homotopy problem departing from this "easy" solution.

The interest is to solve the PFP from an estimate $\mathbf{x}^{(0)}$. Then, the idea is to adjust a fictitious admittance (case of PQ bus) or conductances (case of PV-type bus), which allows us to obtain a solution $\mathbf{x}_* = \mathbf{x}^{(0)}$ when the estimate $\mathbf{x}^{(0)}$ is assigned for the search of the root of $\mathbf{f}(\mathbf{x}) = \mathbf{0}$ in (3.12). The aim is to set a compensation network in such way that the solution is identical to the own initial estimate.

Let $\mathbf{x}^{(0)}$ be an estimate of the flat start type for the set of nonlinear equations in (3.10) and (3.11) for the NR method. i.e., all phase angles are zero, and the voltage magnitude at the PQ bus is equal to 1. The voltage magnitudes at controlled bus $\#k$ are kept constant and equal to V_{0k}. The converged solution in this situation when it occurs is verified for $\mathbf{x}_*$, which is the network state to balance power generations, loads, and losses in the grid.

Now, suppose we connect a compensation shunt admittance $y_k = g_k + jb_k$ at bus $\#k$ of PQ-type of the same network and conductance $y_k = g_k$ at the bus $\#k$ of PV-type. First, the interest is to impose a known solution to the set of equations (3.10) and (3.11) through the introduction of the compensated admittance. Second, the solution should be fitted in such a way that it coincides exactly with the initial estimate $\mathbf{x}^{(0)}$. This implies that the deviations $\Delta\mathbf{x}^{(i)}$ in (3.19) must be zero for any iteration i. Therefore, the solution of the PFP satisfies $V_k = 1$ for PQ buses and $V_k = V_{0k}$ for PV buses, where V_{0k} is the controlled voltage magnitude at the PV buses or slack bus and all phase angles are zero.

For illustration, consider the schematic diagram of a power system model in Fig. 4.1.

Considering the bus $\#k$ as PQ buses, and flat start voltage initialization at bus $\#k$, $\#m$ and $\#j$, $\overline{V}_k = \overline{V}_j = 1.0\angle 0^\circ$ and $\overline{V}_m = V_{0m}\angle 0^\circ$. V_{01} is the voltage in the slack bus. Therefore, the general set of nonlinear mismatch equations in bus $\#k$ for PQ-type, in equation (3.10) and (3.11) will be given by the power injection formulation below.

$$\Delta P_k = P_k - V_k V_j \left[G_{kj}\cos(\theta_{kj}) + B_{kj}\sin(\theta_{kj})\right] - V_k V_{01}\left[G_{k1}\cos(\theta_{k1}) + B_{k1}\sin(\theta_{k1})\right] -$$

$$-V_k V_{0m}\left[G_{km}\cos(\theta_{km}) + B_{km}\sin(\theta_{km})\right] - V_k V_k\left[G_{kk}\right] \tag{4.1}$$

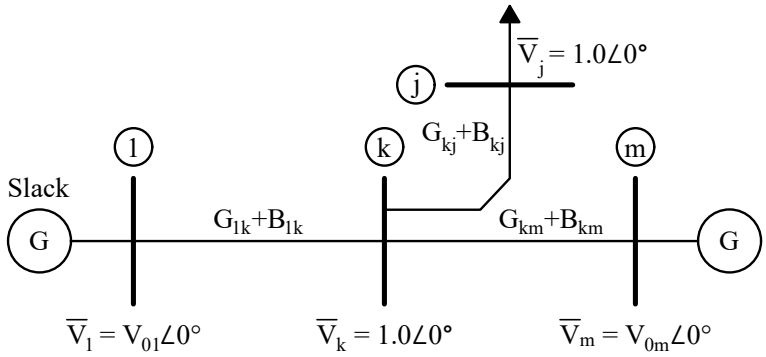

Figure 4.1: Schematic diagram to determine the power flow equations at a bus $\#k$ (PQ-type) - First iteration with flat start point

$$\Delta Q_k = Q_k - V_k V_j \left[G_{kj}\sin(\theta_{kj}) - B_{kj}\cos(\theta_{kj})\right] - V_k V_{01}\left[B_{k1}\sin(\theta_{k1}) - B_{k1}\cos(\theta_{k1})\right] -$$

$$-V_k V_{0m}\left[G_{km}\sin(\theta_{km}) - B_{km}\cos(\theta_{km})\right] - V_k V_k\left[-B_{kk}\right]. \tag{4.2}$$

Handling the equations (4.1) and (4.2) with $V_k = V_j = 1$, $\sin(\theta_{kj}) = \sin(\theta_{km}) = \sin(\theta_{kk}) = 0$ and $\cos(\theta_{kj}) = \cos(\theta_{km}) = \cos(\theta_{kk}) = 1$

$$\Delta P_k = P_k - G_{kj} - V_{01}G_{k1} - V_{0m}G_{km} - G_{kk} \tag{4.3}$$

$$\Delta Q_k = Q_k + B_{kj} + V_{01}B_{k1} + V_{0m}B_{km} + B_{kk}. \tag{4.4}$$

Note that in (4.3) and (4.4), the mismatches ΔP_k and ΔQ_k are not necessarily zero at all. However, we can add a shunt admittance in the bus $\#k$, $y_k = g_k + jb_k$ and set the mismatches zero. This shunt admittance modifies only the terms G_{kk} and B_{kk} in the matrix Y_{BUS}. This works as we have a modified term $G'_{kk} = G_{kk} + g_k$ and $B'_{kk} = B_{kk} + b_k$. Then, the new expressions including the fictitious shunt admittance in the bus $\#k$ are

$$\Delta P_k = P_k - G_{kj} - V_{01}G_{k1} - V_{0m}G_{km} - (G_{kk} + g_k) \tag{4.5}$$

$$\Delta Q_k = Q_k + B_{kj} + V_{01}B_{k1} + V_{0m}B_{km} + (B_{kk} + b_k). \tag{4.6}$$

Therefore, imposing the condition for null mismatches, the compensated admittance values at PQ buses can be adjusted as g_k (4.7) and b_k (4.8)

$$g_k = P_k - G_{kj} - V_{01}G_{k1} - V_{0m}G_{km} - G_{kk} \tag{4.7}$$

$$b_k = -(Q_k + B_{kj} + V_{01}B_{k1} + V_{0m}B_{km} + B_{kk}). \tag{4.8}$$

The same way, considering the bus $\#k$ as PV type as illustrated in the scheme of Fig. 4.2, and flat start voltage initialization at bus $\#k$, $\#m$ and $\#j$, $\overline{V}_k = V_{0k}\angle 0°$, $\overline{V}_j = 1.0\angle 0°$ and $\overline{V}_m = V_{0m}\angle 0°$, the general set of nonlinear equations in bus $\#k$ for PV-type, in equation (3.10) will be given by the power injection formulation below.

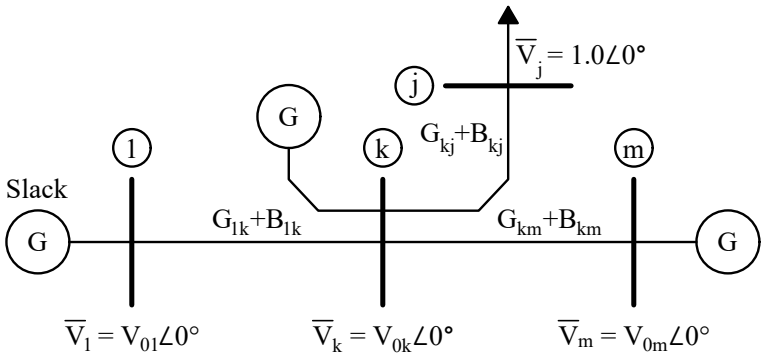

Figure 4.2: Schematic diagram to determine the power flow equations at a bus $\#k$ (PV-type) - First iteration with flat start point

$$\Delta P_k = P_k - V_{0k}V_j\left[G_{kj}\cos(\theta_{kj}) + B_{kj}\sin(\theta_{kj})\right] - V_{0k}V_{01}\left[G_{k1}\cos(\theta_{k1}) + B_{k1}\sin(\theta_{k1})\right] -$$

$$-V_{0k}V_{0m}\left[G_{km}\cos(\theta_{km}) + B_{km}\sin(\theta_{km})\right] - V_{0k}V_{0k}G_{kk}. \tag{4.9}$$

Manipulating the equations (4.9) and with $V_j = 1$, $\sin(\theta_{kj}) = \sin(\theta_{km}) = \sin(\theta_{kk}) = 0$ and $\cos(\theta_{kj}) = \cos(\theta_{km}) = \cos(\theta_{kk}) = 1$

$$\Delta P_k = P_k - V_{0k}G_{kj} - V_{0k}V_{01}G_{k1} - V_{0k}V_{0m}G_{km} - V_{0k}V_{0k}G_{kk}. \tag{4.10}$$

Therefore, the compensated admittance values at PV buses can be adjusted setting $G'_{kk} = G_{kk} + g_k$ and the new expression including the fictitious shunt admitance in the bus $\#k$ is

$$\Delta P_k = P_k - V_{0k}G_{kj} - V_{0k}V_{01}G_{k1} - V_{0k}V_{0m}G_{km} - V_{0k}^2\left(G_{kk} + g_k\right). \tag{4.11}$$

In the same way, imposing the condition for null mismatches at PV-type, g_k can be adjusted as (4.12)

$$V_{0k}^2 g_k = P_k - V_{0k}G_{kj} - V_{0k}V_{01}G_{k1} - V_{0k}V_{0m}G_{km} - V_{0k}^2 G_{kk}$$

$$g_k = \frac{P_k}{V_{0k}^2} - \frac{1}{V_{0k}}G_{kj} - \frac{V_{01}}{V_{0k}}G_{k1} - \frac{V_{0m}}{V_{0k}}G_{km} - G_{kk}. \tag{4.12}$$

In order to compute the fictitious admittances for the compensated network, a generalization for any system can be addressed for the mismatch equations as follows. For a PQ-bus

$$\Delta P_k = P_k - \sum_{\substack{j\in\Omega_{PQ}\\ j\neq k}} G_{kj} - V_{01}G_{k1} - \sum_{\substack{m\in\Omega_{PV}\\ m\neq k}} V_{0m}G_{km} - (G_{kk} + g_k), \quad k \in PQ \tag{4.13}$$

$$\Delta Q_k = Q_k + \sum_{\substack{j\in\Omega_{PQ}\\ j\neq k}} B_{kj} + V_{01}B_{k1} + \sum_{\substack{m\in\Omega_{PV}\\ m\neq k}} V_{0m}B_{km} + (B_{kk} + b_k), \quad k \in PQ \tag{4.14}$$

and for a PV-bus

$$\Delta P_k = P_k - V_{0k}\sum_{\substack{j\in\Omega_{PQ}\\ j\neq k}} G_{kj} - V_{0k}V_{01}G_{k1} - V_{0k}\sum_{\substack{j\in\Omega_{PV}\\ m\neq k}} V_{0m}G_{km} - V_{0k}^2(G_{kk} + g_k), \quad k \in PV \tag{4.15}$$

where Ω_{PQ} and Ω_{PV} represent a set of PQ and PV buses, respectively.

When PQ buses are considered, (4.13) and (4.14) are used simultaneously. However, when bus $\#k$ is of type PV, only (4.15) is necessary. Hence, imposing mismatch equal zero, the compensated admittance values can be adjusted as follows:

$$g_k = P_k - \sum_{\substack{j\in\Omega_{PQ}\\ j\neq k}} G_{kj} - V_{01}G_{k1} - \sum_{\substack{m\in\Omega_{PV}\\ m\neq k}} V_{0m}G_{km} - G_{kk}, \quad k \in PQ \tag{4.16}$$

$$b_k = -\left(Q_k + \sum_{\substack{j\in\Omega_{PQ}\\ j\neq k}} B_{kj} + V_{01}B_{k1} + \sum_{\substack{m\in\Omega_{PV}\\ m\neq k}} V_{0m}B_{km} + B_{kk} \right), \quad k \in PQ \tag{4.17}$$

$$g_k = \frac{1}{V_{0k}^2}\left(P_k - V_{0k}\sum_{m=1}^{N_b} V_{0m}G_{km} \right), \quad k \in PV. \tag{4.18}$$

The fictitious shunt compensation powers inserted in the network are assumed to be of the *constant impedance load type* in such a way that they modify only the full diagonal of the original bus admittance matrix. We discard insertion of this compensation at the slack

bus, because the interest is the state computation at PQ- and PV-type bus.

However, the main objective is to calculate the solution of the PFP formulated according to (3.10) and (3.11). Therefore, the network of compensation needs to be completely removed. This de-insertion can be carried out gradually until it is totally disconnected. The idea is that as progressive withdrawal from the network occurs, PFP solutions are calculated and used for the subsequent phases of the new de-insertion PFP. Evidently, the speed of the associated convergence process depends on the de-insertion rate of the compensation network. This process of gradual removal of the fictitious shunt compensation from the network and calculation of solutions of the PFP at each removal can be carried out by applying a numerical procedure well known as homotopy [7, 11]. In the next section, this problem is discussed and introduced to determine the free compensation PFP solution by considering the flat start guess and the changes in the compensation network previously presented.

4.3 Conclusion of this chapter

In this chapter, the main idea regarding the construction of an initial stage for an estimate of a PFP solution was addressed. The purpose is to insert a fictitious network composed of shunt admittances at PQ- and PV-bus of the system. Since these shunt admittances are inserted to allow the NR method starting from a flat start estimation, they need to be removed in steps such that in the last stage the original PFP solution is reached. The objective is to use the partial solutions in the intermediate steps as initial estimate for the ones subsequent until the final stage.

The computations of the compensation shunt admittance are based on mismatch of the power equations (3.7) and (3.8). In this case, there are distinction between PV- and PQ-bus. By imposing null mismatch on all buses for the initial iteration, the value of the compensation admittances is adjusted. An important aspect of this adjustment is that it is necessary to change only the elements of the main diagonal of the $\mathbf{Y}_{bus}$ matrix.

In the next chapter, it is shown that the construction of the fictitious network presented in this chapter is implemented as the "easy" stage on a homotopy method to compute a PFP solution.

Chapter 5

The Guided Solution by Homotopy Method

5.1 Introduction

This section introduces the Guided Solution by Homotopy - Newton-Raphson (GSH-NR) solver addressed to obtain the PFP solution through a state homotopy path controlled by a proper fictitious network compensation insertion and withdrawal.

Homotopy methods are robust numerical techniques applied for solving systems of non-linear algebraic equations as (3.12) [15, 38]. They are also called numerical path-following methods since they depend on a path emanating from an initial state to a final equilibrium point. The problem consists in designing an appropriate parameterized nonlinear equations system for a parameter $h \in [0, 1]$. The formulation takes into account that at the initial state, defined for $h = 0$, the problem is "easy" to solve or has a known solution, while at the final state, for $h = 1$, it is identical to the "difficult" problem formulated for finding the roots of $\mathbf{f}(\mathbf{x}) = 0$ [38].

In this work, the homotopy process is formulated assuming the inclusion of parameters to gradually modify a fictitious network compensated (formulation for the "easy" problem, which has a trivial solution) modifying it until the original network is recovered (the "difficult" problem, which corresponds to find the zeros of (3.12)), i.e., free of the fictitious network compensated. We also assume that the trivial solution of the "easy" problem is exactly equal to the initial estimate for solving the NR problem at this stage of the homotopy path. This way, the terms (4.16), (4.17) and (4.18) can straightforwardly be computed. The trivial solution considered in the problem is the flat start estimate. However, any other type could be imposed.

5.2 Inclusion of a fictitious network

The homotopy technique applied to a specific problem depends on a homotopy map $\mathbf{G}$ based on the original system of equations $\mathbf{f}(\mathbf{x}) = 0$ according to [7]:

$$\mathbf{G}(\mathbf{x}, \mathbf{h}) = \mathbf{f}(\mathbf{x}, \mathbf{h}) \tag{5.1}$$

where $\mathbf{h} = [h_1 \ h_2 \ \dots \ h_q]^T$ is the continuation parameter set; a map $\mathbf{G}$ is defined as $\mathbf{G} : \mathbb{R}^{n+n_h} \mapsto \mathbb{R}^n$. $\mathbf{h}$ is an independent variable such that $\mathbf{G} : \mathbb{R}^n \times \mathbb{R}^{n_h} \mapsto \mathbb{R}^n$, where in this work we assigned $n_h = 2$. Therefore, the content of $\mathbf{f}(\mathbf{x}, \mathbf{h})$ is adequately modified according to how the homotopy process is implemented in (3.12) and incorporating the changes promoted by the parameters h_1 and h_2 as explained in the sequence.

We propose implicitly defining the map $\mathbf{G}$ as follows. The parameters h_1 and h_2 are used to modify

- the admittance matrix of the system, which initiates with a fictitious value and finishes with its own original value at the end of the homotopy process;
- the value of impedances connecting the slack bus to all other adjacent ones to this bus or, alternatively, other buses at the slack bus' neighborhood.

The intended changes produce an analogous formulation similar to the "continuation power flow" problem with two-continuation parameters. Suppose initially a 1-parameter homotopy problem, where (5.1) and (3.12) are related according to an embedding parameter $h = t$ which is applied for the elements of a modified admittance matrix $\hat{\mathbf{Y}}(t)$. Then (3.10)-(3.11) can be organized in the pattern of (3.12), where now the states $\mathbf{x}$ are dependent on the parameter t. Changes in t leads to

$$d\mathbf{G}(\mathbf{x}, t) = \frac{\partial \mathbf{G}}{\partial \mathbf{x}} d\mathbf{x}(t) + \frac{\partial \mathbf{G}}{\partial t} dt = 0 \tag{5.2}$$

generating the nonlinear system of Ordinary Differential Equations (ODEs)

$$\mathbf{G}_x \frac{d\mathbf{x}(t)}{dt} = -\mathbf{G}_t, \ \ \mathbf{x}(0) = \mathbf{x}_0 \tag{5.3}$$

where $\mathbf{G}_x$ stands for $\mathbf{G}_x = \nabla_x^T \mathbf{G}(\mathbf{x}, t)$ is a Jacobian matrix of the homotopy problem and $\mathbf{G}_t$, for $\mathbf{G}_t = \nabla_t^T \mathbf{G}(\mathbf{x}, t)$ and $\nabla_{\mathbf{x}}(\cdot)$ stands for the gradient operator of $(\cdot)$ for the variable $\mathbf{x}$.

Note that in (5.3), $\mathbf{G}_x$ needs to be nonsingular for all t. Then a homotopy path curve $\gamma(t)$, $0 \leq t \leq 1$, associated with the states at each t, has a finite arc length [38]. Case for some t the Jacobian $\mathbf{G}_x$ is singular (the situation for a saddle-point), the resolution of the problem fails, and the path does not reach the final state at $t = 1$. This introduces an important

aspect of the definition of the homotopy approach applied to the resolution of finding the appropriate solution to the equation $\mathbf{f}(\mathbf{x}) = 0$. However, this fact does not imply that the "difficult" problem has no solution.

Therefore, the homotopy problem can be transformed into a "dynamical" problem [7], also analogous to Newton's continuous problem discussed in the Chapter 3 and proposed in [8, 7, 36] for solving nonlinear equations. The problem can be extended for a multi-parameter homotopy problem, according to the number of parameters defined in $\mathbf{h}$. In this case, a nonlinear Partial Differential Equation (PDE) system should be solved.

Different from the standard Continuation Power Flow Problem (CFP), where a loading factor is changed to modify the system load/generation, in the case of the homotopy exists, only one *physical operation point, which is the last one* determined by solving the "difficult" problem. i.e., the intermediate operation points that are generated according to the "loading factor" $\mathbf{h}$ have no physical meaning. Note that as the physical CFP, the homotopy also has its numerical limitations in relation to the convergence. For instance, the straightforward application of the NR method for this formulation when a saddle-point is reached leads to the failure of convergence [7]. Then, how the homotopy problem formulation is proposed can lead to a "physically" strong (or weak) fictitious network globally. In this sense, our purpose in relation to the implementation of the homotopy problem is to act by modifying only the content of the bus admittance matrix along the homotopy process. This means working only with changes in impedances (admittances), either modifying impedance representing a branch k-m or an equivalent fictitious load/generation. It is demonstrated that the homotopy process can also be interpreted analogously as a nonlinear dynamical problem [7], where a single-homotopy parameter is equivalent to the time t for a generic dynamical system. Consequently, a similar simulation in analogy to the traditional transient stability study in power systems [39] can be applied to evaluate the trajectories of the state path in the homotopy problem. Then, considering these analogies, the original network is modified along the homotopy process proposed in this work, emanating from a flat start guess up to reach a final state when $h_1 = h_2 = 1$. Evidently, how this path is determined will depend on the iterative process adopted and the discretization of the homotopy parameters h_1 and h_2.

Let $\bar{Y}_{kk}$ be a diagonal entry of the original admittance matrix $\mathbf{Y}$. Then, a convex homotopy [15] is adopted as follows. Firstly, the homotopy parameter, h_1, $0 \leq h_1 \leq 1$, is applied to compute a parametric dependent diagonal element as

$$\hat{Y}_{kk} = h_1 Y_{kk} + (1 - h_1)(g_k + jb_k), \;\; k \in PQ. \tag{5.4}$$

For PV-bus, b_k is set to zero. No change is needed for the slack bus. See Fig. 5.1 and 5.2 for an illustration considering fictitious shunt compensation at bus $\#k$. The fictitious shunt elements at the bus are composed of susceptance $b_k^{(1-h1)}$ and conductance $g_k^{(1-h1)}$. The branch element $y_{1k}^{(h2)}$ is controlled by the homotopy parameter h_2, as explained in the sequence.

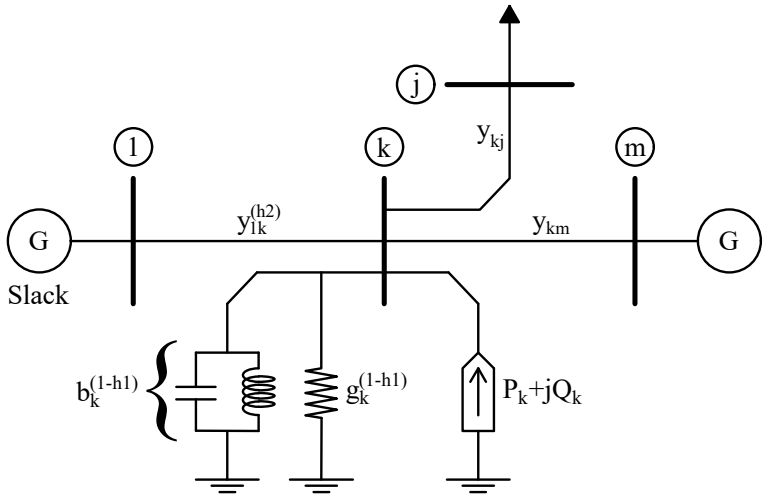

Figure 5.1: Network compensation example by applying 2-parameter homotopy h_1 and h_2 and detailing the resulting circuit at a bus $\#k$ of the type PQ

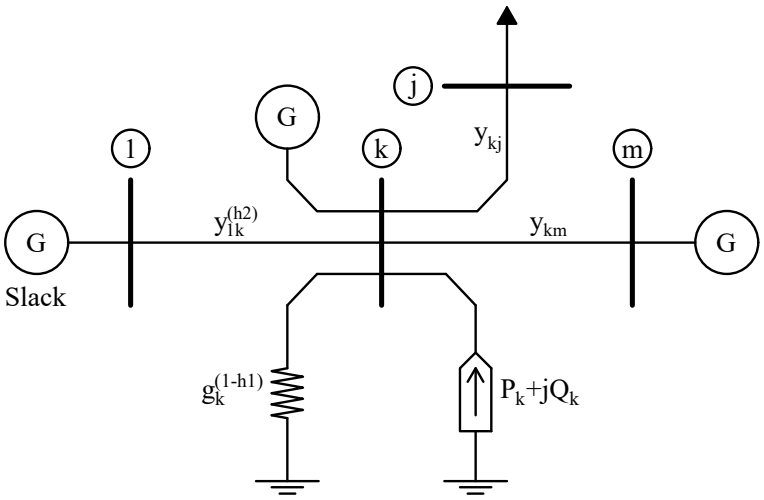

Figure 5.2: Network compensation example by applying 2-parameter homotopy h_1 and h_2 and detailing the resulting circuit at a bus $\#k$ of the type PV

Secondly, the parameter h_2 is used to modify the admittances (or impedances) of the branches connecting buses at the slack bus neighborhood Ω_s. This parameter acts by changing the branch admittance value $y_{km} \in \Omega_s$ connecting the bus $\#k$ to $\#m$. We propose changes in such a way that an updating in the branch admittance can be performed as

$$\hat{y}_{km} = h_2 y_{km} + (1 - h_2)\delta y_{km}, \;\; y_{km} \in \Omega_s \tag{5.5}$$

where a scaling factor δ is adopted to "physically" reinforce the interconnections at the neighborhood of the slack bus along the homotopy process. An artificial strategy of this nature

aims to turn the region near the slack bus stronger and offer a “higher transmission capacity” [39] for the respective links along with the homotopy process. This way, it is expected that the transmission links that connect the slack bus have a wide range of power variation flexibility. This can be useful not only during PFP execution but also throughout the homotopy process. Remember that this can be seen as a "dynamic" process and that it is, therefore, subject to the effect of high nonlinearities throughout the simulation when varying the homotopy parameter in the range [0,1]. We emphasize that the scaling-factor is entirely removed when h_2 reaches the unitary value. Fig. 5.3 exhibits a schematic illustrating a set of buses defined for a region Ω_s. The links in the region include up to two links beyond the slack bus (see interconnections highlighted in red).

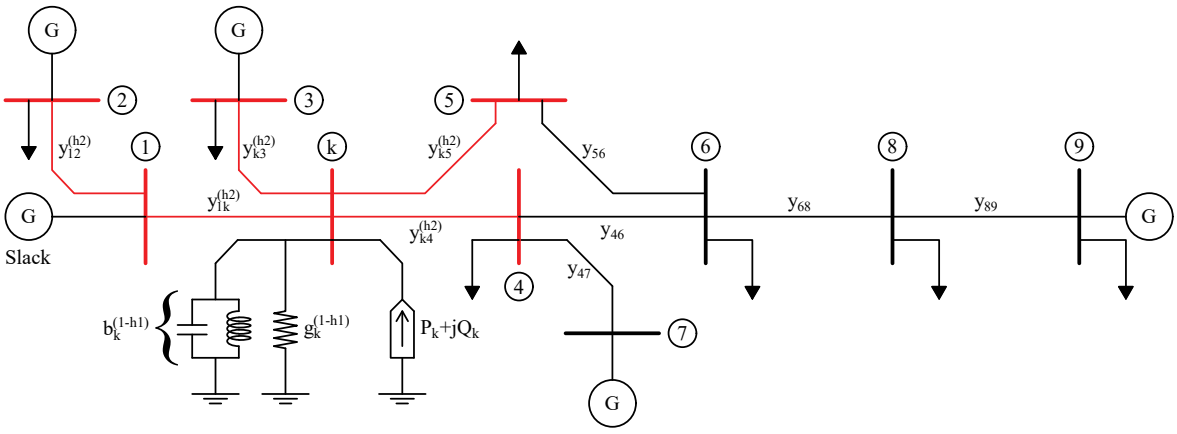

Figure 5.3: Network compensation example by applying 2-parameter homotopy h_1 and h_2 and detailing the resulting compensation circuit at a bus $\#k$ of type PQ and using the scaling factor δ for all the interconnection near slack bus (red color in the sketch)

The purpose is to handle only the reactance value of the impedances, $z_{km} = r_{km}+jx_{km} = 1/y_{km}$, since, in general, the resistances have small values. The strategy consists of reducing (keeping, in the worst case) the reactance values by a positive factor $\delta \leq 1$ to elevate the capacity of the transmission links at the region, Ω_s, in the neighborhood of the slack bus. Consequently, if the reactances of the original interconnection are $x_{km},\ k = 1, 2, \ldots, n_k$, ($n_k$ is the number of transmission links connecting buses $\#k$ and $\#m$), then $\delta \cdot x_{km}$ is the modified reactance by the factor δ. Finally, the second parameter of homotopy, h_2, is set to modify this fictitious reactance while $h_1 < 1$. This generates a fictitious branch impedance

$$\hat{z}_{km} = r_{km} + j[h_2 x_{km} + (1 - h_2)\delta x_{km})]. \tag{5.6}$$

The scaling factor δ is a user-defined parameter, while we set the homotopy parameter h_2 assuming only two natural values, 0 or 1. Hence, the parameter h_2 acts as a switch to activate or not the inclusion of δ, while the parameter h_1 varies. For the experiments, empirically, a unitary value for δ is always adopted on starting a homotopy process. In case of divergence,

the value is reduced to 50%. If the divergence is kept, the last value is reduced again in 50%. This process goes on up to reach a minimum threshold δ^{min}. Each time the scaling factor is modified, a loop involving the computations due to changes in h_1 needs to be carried out in the range $[0, 1]$. Therefore, an iterative problem established this way can be viewed as a two-loop procedure consisting of an external loop for the variation of δ and an internal loop involving steps dependent on changes in h_1.

Finally, considering

- the inclusion of the fictitious shunt admittances for modifying a diagonal entry $\hat{Y}_{kk}$; and
- the value of branch admittances $\hat{y}_{km} = 1/\hat{z}_{km} \in \Omega_s$,

an updated admittance matrix $\hat{Y}$ is calculated with the changes promoted by h_1 and h_2 and used for the execution of the PFP via NR method. This result produces a state $\mathbf{x}_{new}^{(h1,h2)}$ from the initial estimate (previous state) $\mathbf{x}_{old}^{(h1,h2)}$ in case of convergence of the NR method.

5.3 The NR-based solver

The polar representation for voltages and mismatches of power (see (3.10)-(3.11)) are used to determine the PFP solution via homotopy as proposed in this work. The standard NR method is the one employed to compute each state driven according to the homotopy path. Hence, we denominated this strategy as GSH-NR.

Since the parameter h_2 assumes a binary value, the states along the path are controlled by the parameter h_1, for a given value of the scaling factor δ and according to $h_2 = 0$ (or 1). In this work, we adopted a constant step Δh_1, in such a way that the embedding parameter h_1 is updated as $h_1^{(k+1)} = h_1^{(k)} + \Delta h_1,\ k = 0, 1, \cdots, N-1$, where N is the number of steps for the discretization of h_1 in the range $0 \leq h_1 \leq 1$.

Let k be an index for a point of the homotopy path. For this point, if we define $h_1^{(k)}$, then $\bar{\mathbf{x}}_0^{(k)}$ is an initial estimate for the variable $\mathbf{x}$ at the path point k, while $\bar{\mathbf{x}}^{(k)}$ is the determined (converged) state by the NR method at the point k. The process starts with $h_1^{(0)} = 0$, which it is associated with the initial estimate $\bar{\mathbf{x}}_0^{(0)}$ leading to the trivial solution $\bar{\mathbf{x}}^{(0)} = \bar{\mathbf{x}}_0^{(0)} = \mathbf{x}_0$.

The resolution of the NR method along the homotopy path starts with the "easy" problem solution $\bar{\mathbf{x}}^{(0)}$. This result is used as an initial estimate for the computation of the path state at the next point. i.e, $\bar{\mathbf{x}}_0^{(1)} = \bar{\mathbf{x}}^{(0)}$. The process goes on to a generic path point $k+1$ in such way that $\bar{\mathbf{x}}_0^{(k+1)} = \bar{\mathbf{x}}^{(k)},\ k = 0, 1, 2, \cdots, N-1$. In the case of convergence for all N points, the solution of PFP was found. Case a divergence of the NR occurs along the homotopy path, the computations are interrupted, and a new strategy of searching for a converged solution is initiated, considering two possible alternatives. The first one is simply to reduce step

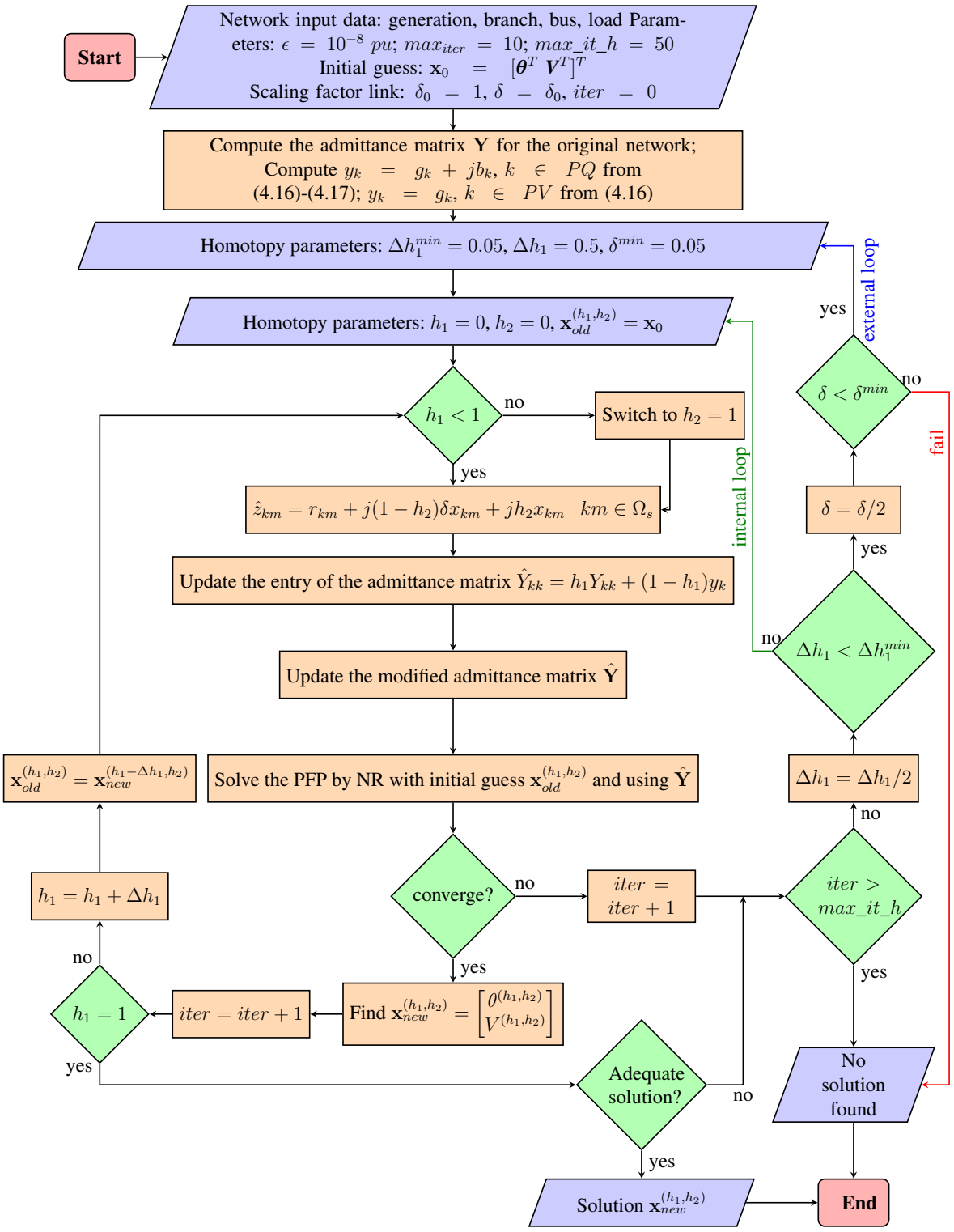

Figure 5.4: Flowchart illustrating the main procedure aspects of the GSH-NR solver for solving the PFP

Δh_1 and restart the "dynamic" simulation in the embedding parameter h_1 (internal loop). A second option, in case the reduction of the step fails, is to reduce the scaling factor δ and restart the "dynamic" simulation involving h_1 (external loop). Case these two alternatives still fail, we consider that the iterative problem diverges.

Figure 5.4 illustrates a flowchart for the computation of the PFP following the

methodology for the GSH-NR solver. The numerical resolution of the homotopy problem aiming to obtain the PFP solution begins with the initialization of variables, parameters, and establishment of thresholds for some parameters. The tolerance for the convergence of the PFP for all homotopy steps is $\epsilon = 10^{-8}$ pu of power; max_{iter} is the maximum number of iterations for convergence of the NR method; while max_it_h controls the maximum number of iterations allowed for solving the homotopy problem. The scaling factor for a link in Ω_s is always initiated with $\delta_0 = 1$. Δh_1^{min} is the minimum step acceptable to discretize h_1, while Δh_1 is a constant step adopted along with the discrete computation of the homotopy path. Since the scaling factor δ is defined, starting with the value δ_0, the internal loop corresponding to the steps for the discretization of h_1 is performed. This internal loop goes on up to h_1 reaches the unitary value. At this step, h_2 is switched from 0 to 1, indicating that the last NR problem will be solved, and a possible final solution of the PFP is searched. Even in case of success for convergence, the result needs to be checked whether it is adequate considering the voltages. For this verification, it is followed the definition in [16]. According to [16], a "correct physical solution" can be acceptable, case the system voltages are in a usually acceptable interval and the angle differences between two connected adjacent nodes are less than 90°. In case of fail, the simulation is restarted initially by reducing the step length Δh_1 until the minimum value if necessary; else, the external loop begins with a reduced scaling factor δ and the step length Δh_1 original. Even so, case none of these interventions leads to success, we consider that the iterative process diverges and the execution must be interrupted.

At each step in the flowchart, the NR method uses an initial estimate $\mathbf{x}_{old}^{(h1,h2)}$, which for $h_1 = 0$ corresponds to $\mathbf{x}_{old}^{(h1,h2)} = \mathbf{x}_0$. The value $\mathbf{x}_{new}^{(h1,h2)}$ is the converged solution for the steps h_1 and h_2. This value will be assigned to the next $\mathbf{x}_{old}$ variable, which will be the initial estimate for the computation of the variable $\mathbf{x}_{new}$. In general, the NR method converges in mean with 3 to 4 iterations at each step for h_1. However, very small step length Δh_1 will require a large number of discrete points and consequently a large number of iterations up to reach the final solution of the PFP. Some works using the homotopy approach initially adopt a large number of discrete points and reduce it along the iterative process according to the convergence. In this work, we have kept constant the step Δh_1 along with a search and modified it according to the flowchart shown in Fig. 5.4.

Simulations are developed and detailed in the sequence to verify the performance of the proposed approach.

5.4 Conclusion of the chapter

This chapter presented the central methodology proposed in this work. The method of calculating the solution to the power flow problem was explained based on the homotopy method. The main contribution was to develop a PFP solution from intermediate solutions

obtained along the path of the homotopy process. These intermediate solutions are used as initial conditions for the subsequent ones. In this way, we start with estimation from a flat start solution ("easy" solution) until reaching the final solution ("difficult" solution). The elements of a fictitious network (see Chapter 4 for setting of this fictitious network) along the homotopy process are modified through a first homotopy parameter. In addition, a second homotopy parameter is used to reinforce the links close to the slack bus. However, in the last stage of the homotopy path, these parameters assume a unit value, signaling the removal of all dummy links. Thus, the final result of the homotopy process is obtained, which corresponds only to the development of the original PFP.

In the following chapter, experiments are carried out, and the respective results are presented in order to demonstrate the effectiveness of the methodology proposed in this work.

Chapter 6

Experiments and Results

6.1 Introduction

This section aims to present experiments in power system models of different scale sizes with the objective of demonstrating the efficacy of the homotopy-based approach proposed in this work to solve the PFP. The results are compared with those ones obtained from simulations carried out by using other numerical techniques or approaches for calculating a PFP solution. All tests are carried out in the MATPOWER tool [40] and by employing adaptation in its native code to implement the homotopy-based problem. The MATPOWER's case database was accessed with its vast set of benchmarks and used for performing the simulations. We have considered all test systems which present divergence for the standard NR for an initial estimate of the flat start type.

The following cases from the MATPOWER's database and also studied in [41] were used to assess simulations aiming to evaluate the impact of the initial estimate on the methods: `case1888rte`, `case1951rte`, `case3012wp`, `case3375wp`, `case6515rte`, `case13659pegase`, and `case_ACTIVSg70k`. Besides that, two smaller test systems, `case9` and `case300`, were investigated to demonstrate the effect of the homotopy-based technique for well-conditioned models. i.e., simulations whose initial estimate of type flat start also converge to the standard NR method. The data for each one of the test systems can be accessed in [42] and the main physical characteristic of the systems are summarized in Tab. 6.1.

Both the database and code were properly adapted to allow the simulations and the implementation of the method based on homotopy, as described in this work. In this sense, for convenience, the first data line in the bus data case files must be assigned to the slack bus, as well as the first data line on the generator data. Therefore, we ensure that the slack bus will always be the first one on the bus labels, considering reference, PQ and PV buses. Also, only one slack bus is assumed.

Several methods have a particular script in the MATPOWER tool [40]. We have used the

Table 6.1: Main physical characteristics of the studied cases

CASE	Number of elements						
	Buses	Generators	Committed Gens	Loads	Shunts	Branches	Transformers
3	3	1	1	2	0	2	0
9	9	3	3	3	0	9	0
300	300	69	69	201	29	411	107
1888rte	1,888	296	290	1,000	45	2,531	2,531
1951rte	1,951	390	365	1,016	24	2,596	2,596
6515rte	6,515	1,368	684	3,673	102	9,037	9,037
3012wp	3,012	502	385	2,271	9	3,572	201
3375wp	3,375	596	479	2,434	9	4,161	383
13659pegase	13,659	4,092	4,092	5,544	8,754	20,467	5,713
ACTIVSg70k	70,000	10,390	8,107	32,460	3,477	88,207	16,855

NR method in its full version to carry out the simulations and compare their results with the homotopy-based approach results. For this situation, simulations were performed with the NR method by considering firstly the initial estimate given in MATPOWER's databank and secondly, an estimate, where a guess of flat start type is imposed.

Additionally, some tests were performed to verify the influence of initial estimates for the PFP solution calculated by the classical NR method. We have always performed the simulations by considering the initial estimate given in MATPOWER's databank and an assessment, where guesses of flat start, DC Power Flow (DCPF), and Gauss-Seidel (GS) types are imposed.

In other words, the purpose is to employ the NR method for an initial estimation and verify its status related to the convergence. In case of divergence, we simply run MATPOWER assuming the initial estimate assigned in its native case file and assume the solution as a reference for comparison with other approaches. For large-scale systems with initial estimate from MATPOWER, convergence via the NR method is successfully obtained. This occurs because the estimate is assigned as an approximation close to the effective solution, as will be verified later in the simulations. In a second simulation, the GSH-NR is employed, *always considering only the initialization of flat start* type.

We perform simulations on ten test systems with 3, 9, 300, 1,888, 1,951, 3,012, 3,375, 6,515, 13,659 and 70,000 buses. Simulations on the smallest test system aim to explain the use of the GSH-NR in a tutorial form. The other simulations were investigated considering the three types of estimates for the NR method, and the results were compared with the reference solution obtained via MATPOWER with its native database estimate.

In the simulations considering the GSH-NR, the trivial solution for the PFP is obtained for $h_1 = 0$ and is equal to the own "flat start" initial estimate. The result is verified because all mismatches are zero and invariant for the initial values of the homotopy parameters h_1 and h_2. At point $h_1 = 1$, the final solution for the PFP is reached in the case of a convergent problem. The application of the procedure highlighted by the flowchart in Fig. 5.4 allows for executing all steps for computations and validation of results.

The GSH-NR method results were then compared to the solution determined by the NR method via MATPOWER, when this latter uses an initial estimate closer to the solution. Additional results were generated based on simulations assessed using other numerical techniques for the resolution of the PFP. Two techniques exploit the philosophy of the Continuous Newton's Method (CNM) as proposed in [7, 8]. Then, considering this idea, we perform simulation on a straightforward approach that uses the Runge-Kutta formula (defined in [8] as classical fourth-order Runge–Kutta formula) (RK4) to solve the CNM; and an implicit formulation of the CNM denominated Implicit CNM (ICNM) [36]. The method uses a Backward Euler integration method to solve the problem. For this last approach, it was implemented the alternative called ICNM-J_1, for which the computation of a Hessian matrix is avoided. A third technique uses a homotopy-based method called Injection Homotopy (IH) [17]. By this approach, an equivalent power is injected at each bus for initiating the homotopy process. Therefore, at this step, the consumption (generation) of the bus is supplied (absorbed) by the own bus. The amount of fictitious power is removed until it disappears entirely at the end of the homotopy process.

Finally, simulations were conducted by considering operational limits of reactive power at the power generations. The goal of these simulations is to demonstrate that the challenge is to compute the initial PFP convergent solution for the operation point free of limits. Then, using this solution as an initial guess for the constrained cases, the convergence is obtained by applying only the standard NR for a few iterations to find the solution with such constraints.

An essential aspect of the GSH-NR solver application is computing the middle path between the initial and the final states. Only the final one needs a high accuracy for the mismatches. Then, considering this argument, we have suggested relaxing the tolerance for a PFP convergence along the path of intermediate states. The fact is justified since the idea is to obtain closer states at each step h_1 until the final equilibrium point is achieved. Based on these fundamentals, we adopted for simulations the power mismatch tolerance $\epsilon = 10^{-8}$ pu for the results of all PFP, except those ones from intermediate states of a homotopy path. In this case, a relaxed tolerance $\epsilon = 10^{-2}$ pu and a maximum of 6 iterations are adopted.

All simulations were performed by using MATLAB R2018a with MATPOWER 6.0 [42]. To provide comparisons of the time results of different computers, the simulations were run on a personal computer, Intel(R) Core(TM) i7-8565U 8th Gen, 256 GB SSD CPU, 1.80 GHz, 8 GB RAM, 64-bit OS.

6.2 Experiments on a 3-bus test-system

Some tests were carried out on a 3-bus test system to illustrate the use of the GSH-NR solver. The one-line diagram of the network is exhibited in Fig. 6.1. The single system is modeled by a slack bus and two equivalent PQ buses. Two interconnections link the buses. Only longitudinal admittances connect the buses. The two loads at buses $\#2$ and

#3 are of type constant power, and their complex values are $\overline{S}_{L2} = 0.70 - j0.30$ pu and $\overline{S}_{L3} = -0.35 - j0.12$ pu, respectively. The admittances linking two buses are y_{12} and y_{23} computed, respectively, as the inverse of the impedances $z_{12} = 0.5 + j0.8$ pu and $z_{23} = 0.5 + j0.9$ pu. The voltage at the slack bus is set $\overline{V}_1 = 1.0\angle 0^o$.

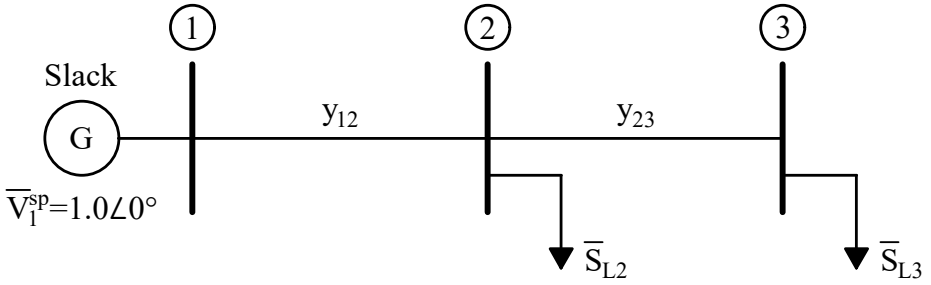

Figure 6.1: One-line diagram for the 3-bus test system

The application of the homotopy process begins with the definition of the pertinent parameters h_1, h_2, δ, g_k and b_k. First, we compute g_k and b_k according to (4.16) and (4.17)

$$\begin{aligned} g_2 &= P_2 - G_{23} - V_{01}G_{21} - G_{22} \\ b_2 &= -\left(Q_2 + B_{23} + V_{01}B_{21} + B_{22}\right) \end{aligned} \tag{6.1}$$

$$\begin{aligned} g_3 &= P_3 - G_{32} - G_{33} \\ b_3 &= -\left(Q_3 + B_{32} + B_{33}\right) \end{aligned} \tag{6.2}$$

knowing that the admitance element $y_{ij} = g_{ij} + jb_{ij} = \dfrac{1}{R_{ij} + jX_{ij}}$, and the element of Y_{bus}, out of the main diagonal, Y_{ij} $(i \neq j)$, is $-y_{ij}$, then

$$\begin{aligned} G_{21} + jB_{21} &= -y_{21} = -\frac{1}{0.5 + j0.8} = -0.562 + j0.899 \\ G_{23} + jB_{23} &= -y_{23} = -\frac{1}{0.5 + j0.9} = -0.472 + j0.849 \end{aligned} \tag{6.3}$$

and the main diagonal of Y_{bus}, $Y_{ij}(i = j)$, consists of the sum of the adjacent elements, as

$$\begin{aligned} G_{22} + jB_{22} &= y_{21} + y_{23} = \frac{1}{0.5 + j0.8} + \frac{1}{0.5 + j0.9} = (0.562 - j0.899) + (0.472 - j0.849) \\ G_{33} + jB_{33} &= y_{23} = \frac{1}{0.5 + j0.9} = 0.472 - j0.849 \end{aligned} \tag{6.4}$$

therefore, according to (6.1) and (6.2)

$$\begin{aligned} g_2 &= -0.70 - (-0.472) - 1.0 \cdot (-0.562) - (0.562 + 0.472) \\ b_2 &= -\left[0.3 + 0.849 + 1.0 \cdot 0.899 + (-0.899 - 0.849)\right] \end{aligned} \tag{6.5}$$

$$\begin{aligned} g_3 &= 0.35 - (-0.472) - 0.472 \\ b_3 &= -\left[0.12 + 0.849 + (-0.849)\right] \end{aligned} \tag{6.6}$$

giving the values $g_2 = -0.70$ pu, $b_2 = -0.30$ pu, $g_3 = 0.35$ pu and $b_3 = -0.12$ pu. These parameters depend only on the configuration and loading of the original network. Then, when the estimated values for the voltages are $V_2^{(0)} = V_3^{(0)} = 1$ pu and $\theta_2^{(0)} = \theta_3^{(0)} = 0^o$, the net load at each bus is zero. Therefore, the result found for the nodal voltages from the power flow resolution for $h_1 = 0$ is trivial and equal to 1.0 pu for all buses. It is worth noting that the complex values for $g_k + jb_k,\ k = 2, 3$ coincide with $-\overline{S}_{L2}^*$ and $-\overline{S}_{L3}^*$ because there is only the slack bus as a controlled voltage source in the system and set for 1,0 pu. In addition, if the voltage on the slack bus were different from 1 pu, the values g_k and b_k would need to be corrected with the assigned voltage at the slack bus, according to expressions (4.16) and (4.17). Likewise, if there were a PV bus, the voltage controlled in the generating bus would also need to be used for correcting g_k and b_k in PQ bus.

The second homotopy parameter h_2 is also associated with the scaling factor δ to modify an impedance z_{km} to $\hat{z}_{km}$, as explained in Section 5. Due to the small size of the model, only the connection 1-2 is chosen to compose the region Ω_s. This means that h_2 is used to switch from the modified bus impedance $\hat{z}_{12}$ to the original impedance z_{12}. Then, the impedance z_{12} will be modified according to the homotopy parameter h_2 as $\hat{z}_{12} = \delta z_{12}$ for $h_1 < 1$, i.e., $h_2 = 0$; or $\hat{z}_{12} = z_{12}$ for $h_1 = 1$, i.e., $h_2 = 1$.

Simulations were carried out by applying the NR method with a flat start estimate to determine the PFP solution. The calculated nodal voltages for buses 2 and 3 were $\overline{V}_2 = 0.909\angle{-32.228^o}$ pu and $\overline{V}_3 = 1.131\angle{-17.859^o}$ pu, respectively. Six iterations were needed to reach the convergence. In this case, the use of the GSH-NR is senseless, given that the standard NR method is adequate to resolve the problem directly. On the other hand, the homotopy method was used to solve the problem and verify how the step Δh_1 and the scaling factor δ influence the computation of the PFP. We emphasize that the straightforward use of the NR method in this study would be sufficient to obtain the PFP solution at the operation point and that the example has a tutorial purpose only.

The simulations involving the homotopy process have considered changes in step Δh_1 for two values, 0.1 and 0.2. For both investigations, it was assigned the values 0.05, 0.1, 0.5, and 1.0 for the scaling factor δ. Fig. 6.2 exhibits the results for nodal voltage magnitude and angle in bus 2 (similar results were also obtained for bus 3 and not shown here). The simulations show that the homotopy parameter h_1 is sensitive to step Δh_1 for small values of δ. When $\Delta h_1 = 0.1$ (see Figs. 6.2.a and 6.2.b), the final state of the homotopy path converges

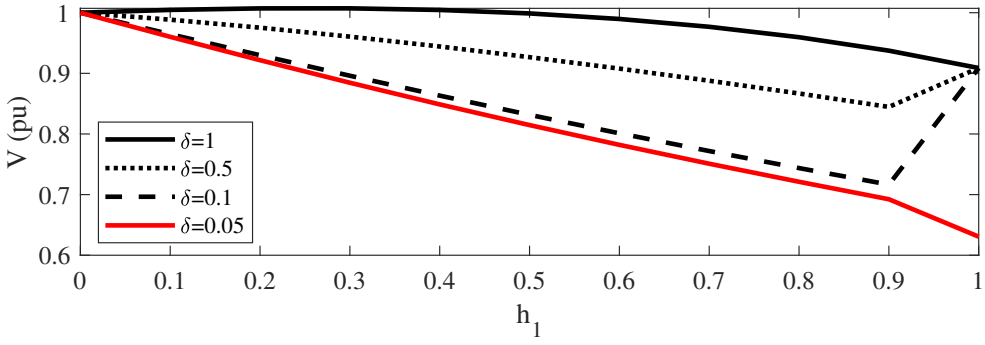

(a) Voltage magnitude for $\Delta h_1 = 0.1$

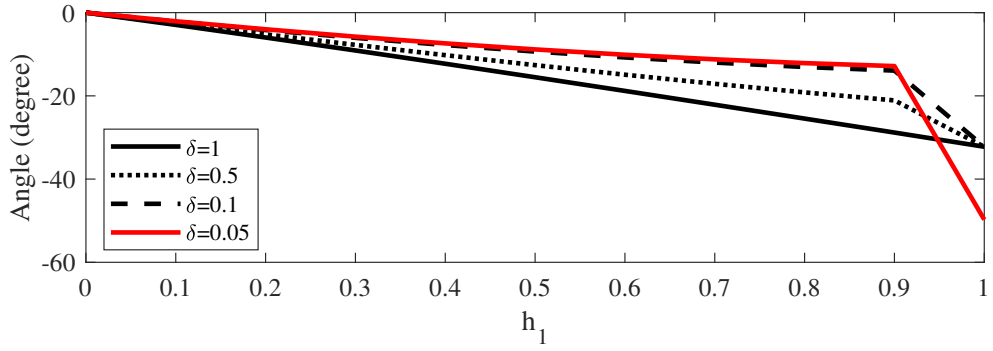

(b) Voltage angle for $\Delta h_1 = 0.1$

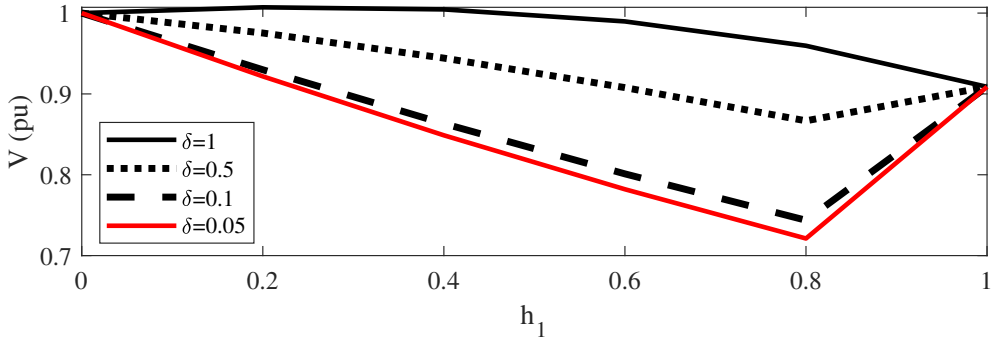

(c) Voltage magnitude for $\Delta h_1 = 0.2$

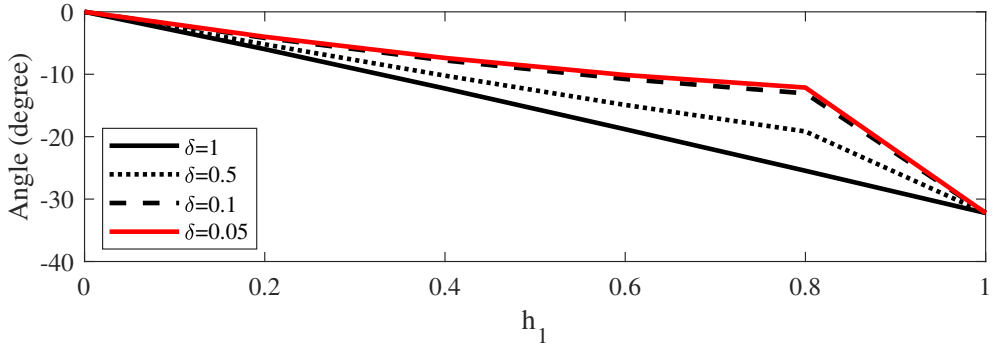

(d) Voltage angle for $\Delta h_1 = 0.2$

Figure 6.2: Trajectories along to the homotopy process, when $\Delta h_1 = 0.1$ (cases (a) and (b)) and $\Delta h_1 = 0.2$ (cases (c) and (d)), of the quantity values of voltage magnitude and angle at bus 2

to a Low Voltage (LV) operation point for $\delta = 0.05$. The value is $\overline{V}_2 = 0.631\angle{-49.73}^o$ pu, which has well smaller magnitude than the High Voltage (HV) $\overline{V}_2 = 0.909\angle{-32.228}^o$ pu, calculated by the MATPOWER's software. Higher values for δ leads to the convergence to HV point, despite it occurring through different paths. An increment in Δh_1 to 0.2 (see Figs. 6.2.c and 6.2.d) reduces the influence of δ on the search for the HV solution, however, it still affects the homotopy path.

Despite the simplicity of the model, we can conclude from the simulations that both Δh_1 and δ affect the homotopy path, and this sensitivity can be significant for some specific power system model.

6.3 Experiments on a 9-bus test system

In this subsection, the results for experiments from a classical 9-bus test system are presented. The data of this small test system were obtained from MATPOWER's databank (`case9.m` file) [37]. When the NR method is applied to solve the power flow problem for the scenario represented by the network, the process is convergent using an initialization flat start. We present these tests to account for this type of process, which is less restrictive for the methodology proposed in this work. Additionally, the reader can follow up on the methodology using a reduced and more accessible system regarding the handling of results. The system has 9 buses, of which, in addition to the slack bus, there are two generation buses and six load buses.

Regarding the homotopy-based method application, we performed simulations by using $\delta = 0.1$. The homotopy parameter h_1 was incremented by a step equal to 0.1. Fig. 6.3 shows the evolution of the voltage magnitudes and phase angles as a function of h_1. Until the value $h_1 = 0.9$, the value h_2 is zero, which indicates that the scaling factor $\delta = 0.1$ is used to reduce the impedance of the interconnection connected to the slack bus. This justifies the jumps on the curves in the interval for h_1 between 0.9 and 1.0 when h_2 jumps to unity. A better refinement could be implemented for h_1, adjusting a smaller step for this interval. However, our empirical results have demonstrated small computational gains in relation to the concern of an additional burden due to the need to run new power flow problems for new values of the parameter h_1.

Other experiments were also performed for $\delta = 0.01$ and $\delta = 0.5$. However, unless the natural changes at homotopy trajectories, the final results agree with those ones found by employing $\delta = 0.1$. All results determined by the homotopy-based approach concerning the final state of the systems are in accordance with those ones found by the traditional NR method.

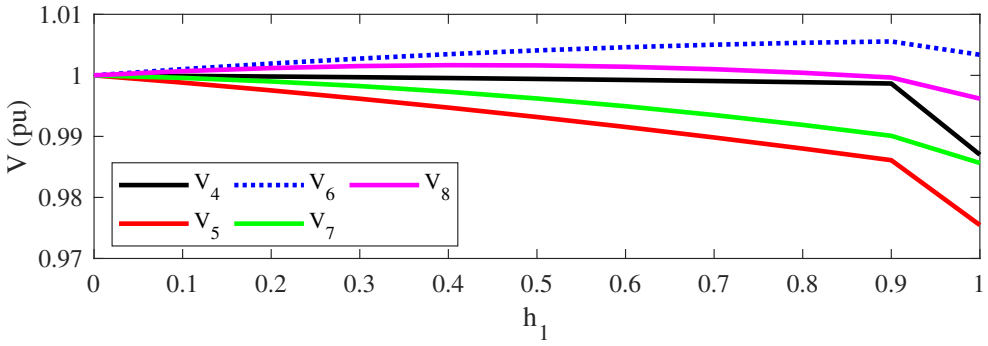

(a) Voltage magnitude

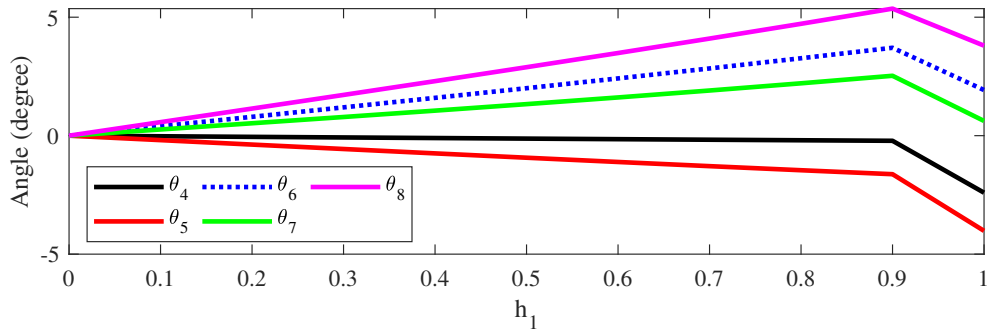

(b) Voltage angle

Figure 6.3: Evolution of the quantity values of voltage (a) and angle (b) with h_1 for the 9-bus system

6.4 Medium to large-scale test system models

This subsection provides a descriptive summary of medium to large-scale test systems used to assess simulations in the remainder of this work. All the test system model data can be found in the MATPOWER's case databank (see additional details in [37]), and any power system can be tuned to fit MATPOWER. In the subsequent studies, the test systems were used to evaluate the performance of the proposed method and compared with the performance of other techniques. The initialization of the NR method is also investigated for alternatives of initial estimate different from the flat start.

6.4.1 300-bus system

The test system is known as the IEEE 300-bus system. It is a synthetic model created by the IEEE Test Systems Task Force in 1993 and is a benchmark widely used for PFP and optimal PFP studies [43]. The PFP running for this test system with the NR method converges for an initial estimate of type flat start. The inclusion in this study is justified to have also results at all for a well-conditioned model.

6.4.2 European RTE models

They are test system models consisting of some equivalent networks of the French high voltage transmission system [44]. Three test systems were used in our simulations, known as `case1888rte.m`, `case1951rte.m`, and `case6515rte.m`. The number of components in each equivalent model, therefore, will depend on the size of the selected model.

6.4.3 Polish model

It consists of models representing the Polish's system during the winter of 2007-08 evening load peak conditions [37]. Two equivalent test systems corresponding to the `case3012wp.m` and `case3375wp.m` (the latter with bus #10,287 isolated) are studied in this work.

6.4.4 13,659-bus Pegase test system

This network base case represents the size and high voltage transmission network of a European equivalent system, including voltages ranging from 110 kV to 750 kV. The model has 13,659 buses, 4,092 generators, and 20,467 branches (see [45] for additional details). All information in relation to the data can be obtained from MATPOWER's databank (`case13659pegase.m`).

6.4.5 Synthetic USA test system

The model presents 70,000 buses and represents a synthetic eastern United States power system model, as presented in [46, 47]. The model is in MATPOWER's databank as file `case_ACTIVSg70k.m`. We have used the same data file, but moving the slack bus data line to the first position at the bus data allocation.

6.5 Simulations on the medium to large-scale test systems

This subsection aims to describe the results of simulations at all eight test systems presented in Subsection 6.4. For all simulations, the equipment's operational limits are assumed free.

The base cases of each test system were evaluated by using the initial estimate set in the MATPOWER's native case databank (NR-MAT). For this condition, they all presented convergence for a solution for running the PFP by using the MATPOWER's solver based on the classical NR, as can be seen at columns eight and nine in Tab. 6.2. Such converged

values are adopted here as the *reference* result for comparison purposes. However, when a flat start estimate is adopted for the MATPOWER's NR solver, just the `case300.m` reached convergence, yielding the expected reference result (see 2nd and 3rd columns). All other cases had divergence for the standard NR solver, as can be seen at columns two and three. Two different forms of establishing an initial guess for the NR solver were evaluated for the test systems. The first one is based on the DC power flow (DCPF) used to compute only voltage angles. A second one is based on two iterations of the Gauss-Seidel (GS) method initializing from a flat start estimate. Tab. 6.2 summarizes aspects of convergence and required iterations for convergence for these conditions. Columns four and five show the status for the initialization by DCPF and the necessary number of iterations (iter) for convergence for the NR solver, respectively. Columns six and seven are similar results for initialization with two iterations of the GS method. The last column presents the number of iterations required for convergence by the NR solver when the MATPOWER's initialization is adopted. Note that for both cases 1888rte and 1951rte, the initialization is the own solution of the PFP.

Even with the initialization with GS, the NR solver cannot correctly solve the PFP to the two most significant models. Additional iterations allowed to the GS method do not improve the NR solver's performance. On the contrary, it causes deterioration of the convergence.

The study was extended to the evaluation aiming for improvements based on the proposed GSH-NR method and three other established approaches. The alternative approaches are based on an Injection Homotopy (IH) [17]; Backward Euler (BE) solver for determining the PFP solution following the implicit continuous Newton's method (CNM) philosophy [36]; and an RK4 solver to assess the PFP solution now with an explicit approach for the CNM philosophy [8]. All simulations considering these techniques assumed a flat start initialization since it was a more rigid form of initialization for the iterative NR-based methods. Besides the initialization, all these techniques are parameter-dependent. The simulation results for the four approaches are given in Tab. 6.3.

The BE method needs the setting of a step α, inserted in column two. This parameter is

Table 6.2: Simulations with initial estimate for the NR computed from different estimate, including the flat start type

	NR guess						NR	
CASE	NR-flat	iter	DCPF	iter	GS	iter	NR-MAT	iter
300	√	5	√	5	√	5	√	5
1888rte	X	-	√	5	√	6	√	1
1951rte	X	-	X	–	√	6	√	1
6515rte	X	-	√	7	√	7	√	2
3012wp	X	-	X	–	√	5	√	3
3375wp	X	-	X	–	√	5	√	4
13659pegase	X	-	√*	6	√*	6	√	5
ACTIVSg70k	X	-	X	–	X	–	√	6

√: convergence; X: divergence;
√*: convergence to a different solution.

equal to Δt as defined in Subsection 3.3.2 In this work, the step is kept constant along with the iterations, whose number for convergence is indicated in column three. The parameters and iterations for the RK4 solver are shown from the fourth column up to the seventh one. The RK's step is usually defined as $h = \Delta t$ (see Subsection 3.3.1). In this work, it will be called α to avoid double definition with the parameter h used in the homotopy context. Then for the RK4 solver, we adopt a constant step α_1 until the iteration $iter_1$. After that, the step is changed to α_2, when the convergence is not obtained for the iteration $iter_1$. It is kept constant for the remainder of iterations. In the seventh column is indicated the global number of iterations for convergence.

The injection homotopy described in [17] was implemented being the homotopy-based method for comparison with the performance of the GSH-NR. It was also carried out an adaptation to include phase-shifter models on the control performed by the homotopy parameter. Without this control, it was verified divergence on several test systems. The implementation of the method is based on the compensation of constant power injection (load/generation) along the homotopy path. Therefore, fictitious generations and loads are connected to the network and removed gradually by the insertion of the homotopy until the final state. We adopt here for this method a homotopy parameter h, which is discretized in steps Δh. The eighth and ninth columns in Tab. 6.3 gives step Δh and the number of iterations required to solve the homotopy problem. Step Δh is set initially in 0.5. In case of divergence, it is reduced by a half until a minimum threshold 0.05. Therefore the number of iterations shown in the table is equal to the number of runs of the NR problem.

The results from the GSH-NR solver are shown from the tenth to the twelfth column. The tenth column exhibits the final step Δh_1, for the discretization of the homotopy parameter h_1. According to the flowchart in Fig. 5.4, the step starts with $\Delta h_1 = 0.5$ and is reduced to a half in case of divergence of the NR method the first time along with the current homotopy path. This fact causes the restart of the computations requiring an updated Δh_1. For this condition, the step is reduced following this strategy until the threshold Δh_1^{min} be reached. Step Δh_1 can reach its low limit. In this case, the scaling factor δ must be reduced (external loop action) by a half and the internal loop that control the variation of h_1 is activated, beginning

Table 6.3: Performance of the GSH-NR and other techniques for simulations on the eight test systems

CASE	BE		RK4				IH		GSH-NR		
	α	$iter$	α_1	$iter_1$	α_2	$iter_2$	Δh	$iter$	Δh_1	δ	$iter$
300	10^4 √	5	1.0 √	2	1.6 √	5	0.5 √	2	0.5 √	1.0	2
1888rte	X	–	X	–	X	–	0.5 √	2	0.25 √	1.0	5
1951rte	X	–	X	–	X	–	X	–	0.25 √	1.0	5
6515rte	X	–	X	–	X	–	0.25 √	6	0.0625 √	1.0	19
3012wp	1.0 √	37	0.1 √	2	1.6 √	6	0.5 √	2	0.25 √	1.0	6
3375wp	1.0 √	37	0.1 √	2	1.6 √	6	0.5 √	2	0.25 √	1.0	6
13659pegase	100 √	9	0.1 √	2	1.6 √	7	0.25 √	6	0.25 √	0.125	19
ACTIVSg70k	0.1 √	259	X	–	X	–	X	–	0.125 √	1.0	11

√: convergence; X: divergence.

Table 6.4: Execution time in seconds for the tests carried out according to Tab. 6.3 (iteration number between parenthesis)

CASE	BE	RK	IH	GSH-NR	NR
1888rte	–	–	0.0415 (2)	0.495 (5)	0.0208 (1)
1951rte	–	–	–	0.550 (5)	0.0338 (1)
6515rte	–	–	0.676 (6)	2.185 (19)	0.1116 (2)
3012wp	0.6187 (37)	0.401 (8)	0.123 (2)	0.4412 (6)	0.0570 (3)
3375wp	0.6902 (37)	0.465 (8)	0.131 (2)	0.458 (6)	0.0764 (4)
13659pegase	0.7304 (9)	2.27 (9)	2.511 (6)	8.19 (19)	0.4425 (5)
ACTIVSg70k	139.7 (259)	–	–	33.77 (11)	3.072 (6)

again from the value $\Delta h_1 = 0.5$. While a complete homotopy path is not concluded, this process continues until the external loop with δ also reaches a minimum value. Therefore, the total number of iterations accounted for in the twelfth column is the sum of all number of NR's solutions necessary to reach the final state on the finite homotopy path search to calculate the PFP's solution.

Remember that an NR solver in the homotopy process "solves a PFP" at each point of the homotopy line search $h_1 \in [0,\ 1]$. Each one of these PFPs presents a mean of 3 to 4 iterations. As we are interested in obtaining the final solution of the PFP (the "difficult" problem) from an initial estimate based on a flat start, the intermediate states of the homotopy path are not physically significant. Therefore, we suggest constraining the maximum number of the NR iterations, max_{iter}, to check convergence and relax the tolerance. For this intermediate point of the homotopy path we have considered at most six iterations, and a tolerance 10^{-2}, which is significantly reduced compared to the tolerance 10^{-8} kept to the computation of the final state.

The execution times for the simulations of the test systems were measured. The same conditions in Tab. 6.3 were considered, assuming all convergent situations. Tab. 6.4 presents the runtime necessary to perform the computations in Tab. 6.3. At the side of the time, between parenthesis, is given the number of iterations which are also verified in Tab. 6.3. As can be seen from both Tabs. 6.3 and 6.4, considering flat start estimation, the GSH-NR and BE solvers are able to resolve the PFP for the most significant test system. However, the BE method demands a high cost when the computational burden is compared. Additionally, while the GSH-NR is able to find a solution to the PFP for all test systems, the BE solver fails to calculate a solution in the case of the RTE's equivalent models. The GSH-NR requires high computational cost compared to the standard NR figure. This is verified because the NR results are obtained from the initial estimate closer to the solution defined in MATPOWER's case databank.

In the sequence, specific studies related to the GSH-NR are performed on the two biggest test model to evaluate the impact of the step Δh_1 and δ, since they are parameters that can affect the convergence of a given test system. An example is found in Tab. 6.3 for the `case13659pegase`, which is affected by both Δh_1 and δ (see tenth to the eleventh column

in Tab. 6.3). We investigated the influence of these parameters on the two biggest test models in the following subsections.

6.6 Experiments on a 13,659-bus system

This subsection provides results for experiments assessed for a large-scale system. The simulations demonstrate the necessity for using the scaling factor δ in the convergence process and the robustness of the method to be guided to the solution when the homotopy-based method is applied. Simulations were carried out on the network base case obtained from MATPOWER's databank (`case13659pegase.m`). The system represents the size and high voltage transmission network of a European equivalent system, including voltages ranging from 110 kV to 750 kV. The model has 13,659 buses, 4,092 generators, and 20,467 branches (see [45] for additional details).

We have performed the simulations with the NR method by considering the initial estimate given in MATPOWER's databank and a second estimate, where an initial estimate of flat start type is imposed. When the initial estimate from MATPOWER is used, the NR method converges. However, for the flat start initialization, the NR method is divergent. The MATPOWER's initial estimate for running the NR method is illustrated in the plots of Fig. 6.4. The solution of the PFP is included in the same plot. We can verify that the solution and initial estimate have very close values. This pattern contributes to the convergence of the NR method.

The application of the homotopy-based method depends on the usual parameters, as done for other experiments described previously. The scaling factor δ was applied for the single impedance between the low and high voltage buses connecting the slack bus (at the low voltage side) according to the homotopy parameter h_2. As usual, a step 0.1 was adopted for h_1. However, concerning the parameter δ, its value can affect the process of convergence. Then, some experiments were performed to verify its impact on the final state results. Considering that the system is ill-conditioned, judging by the divergence of the problem with the flat start type initialization [8], a maximum δ value was investigated to assess its impact on the analysis. This value was determined iteratively, starting with small δ values until reaching a limit for which the state values either diverge or are very different from those previously computed for smaller δ. Then, following this procedure, four situations were analyzed for the values 0.01, 0.1, 0.12, and 0.13.

The plots in Figs. 6.5, 6.6 and 6.7 illustrate curves of trajectories of magnitude and phases of voltages (some states) involving varying aspects δ. The magnitude and angle of voltages at the index of buses $\#461$, $\#3054$, $\#7130$, $\#8575$, and $\#9846$ are monitored. From the voltage magnitude plots, no significant variation is observed. On the other hand, when the analysis involves the phase angles, a big change along the homotopy process is verified, augmenting δ. These elevated values occur mainly in the interval for h_1 between

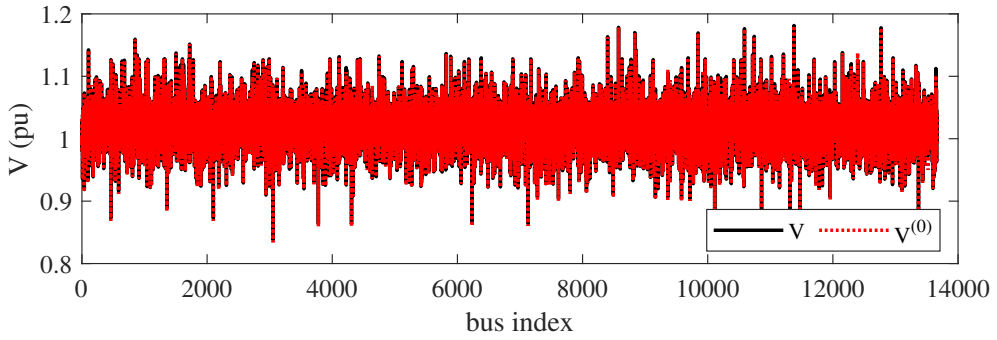

(a) Voltage magnitude

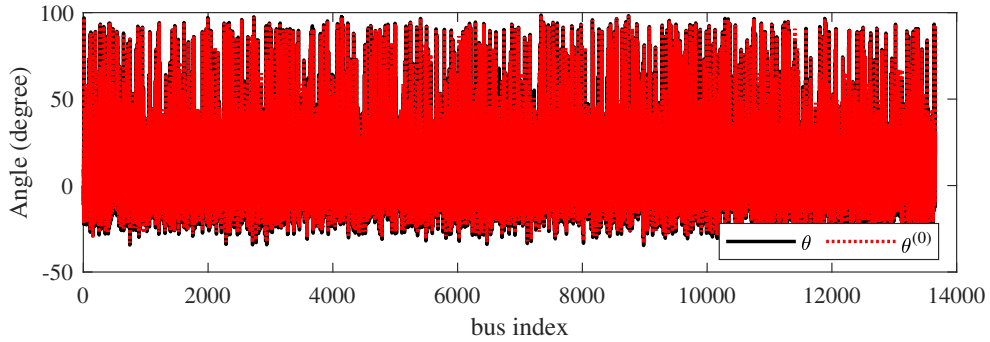

(b) Voltage angle

Figure 6.4: Initial estimation and final states for the 13,659-bus system

0.2 and 0.8. The angle curves are practically continuous for δ until 0.12. From Fig. 6.7.b, which corresponds to the case $\delta = 0.13$, the angles suffer discontinuity. This characteristic indicates that the operation point changed to the other condition in relation to the previous states obtained for smaller values of δ. This is typical of an unstable voltage operation point considering the elevated variation in the phase. In fact, we computed the generation produced by the slack bus for the final homotopy state ($h_1 = 1$), and active and reactive power generation were 0.7687 pu and 0.1581 pu, respectively, for values of $\delta \leq 0.12$. For $\delta = 0.13$, the same generation changed to 1.564 pu and 14.6 pu. When the simulation is carried out for $\delta \geq 0.14$, the process no longer converges.

Another set of tests considered the scaling factor δ, which was also extended to the links connecting the high voltage side of the slack bus. In the previous simulations, the scaling factor δ was applied to only 1 link that connects the slack bus and the high voltage bus side. Therefore, the region Ω_s has just one element. However, other 26 additional links are connected to the high voltage bus. Then, for this new simulation, the impedances of these interconnections were also modified according to δ and h_2. Now, the region Ω_s has 27 elements. Considering this extension, the limit for using δ was increased to 0.37 rather than that of 0.12 obtained without the additional link changes. Therefore, when many weak connections exist with the slack bus (or near it), the strengthening of the links at the neighborhood of the slack bus improves the capacity of power transmission from/to this bus. Then, this temporary and artificial reinforcement provided by acting in the parameter δ works as an

essential source to support a high variation of power during the homotopy process. This is in agreement with the results found in Tab. 6.3, when there $\delta = 0.125$ was used and still sufficient for convergence. On the other hand, when $\delta = 0.13$, the PFP found a solution giving phase difference for some two buses greater than 90^o.

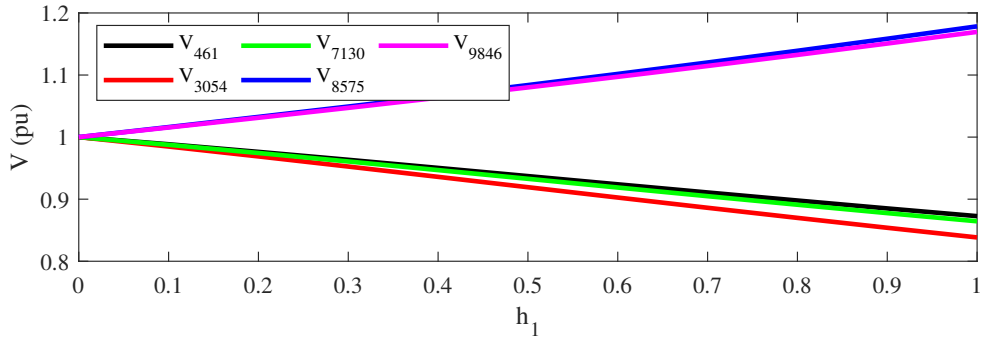

(a) Voltage magnitude, $\delta = 0.01$

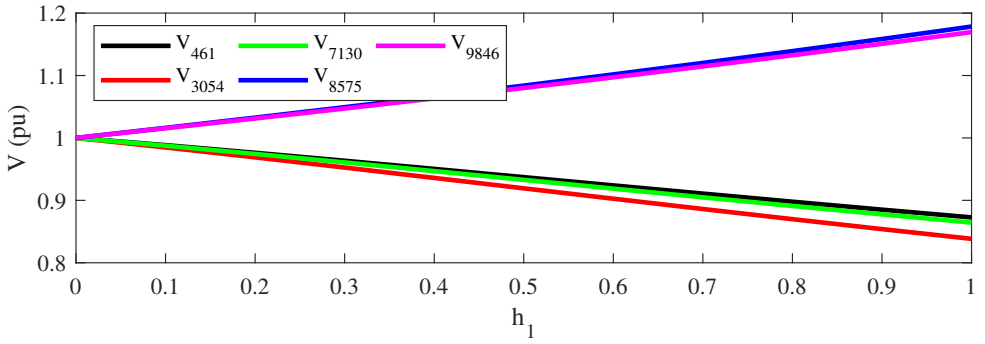

(b) Voltage magnitude, $\delta = 0.1$

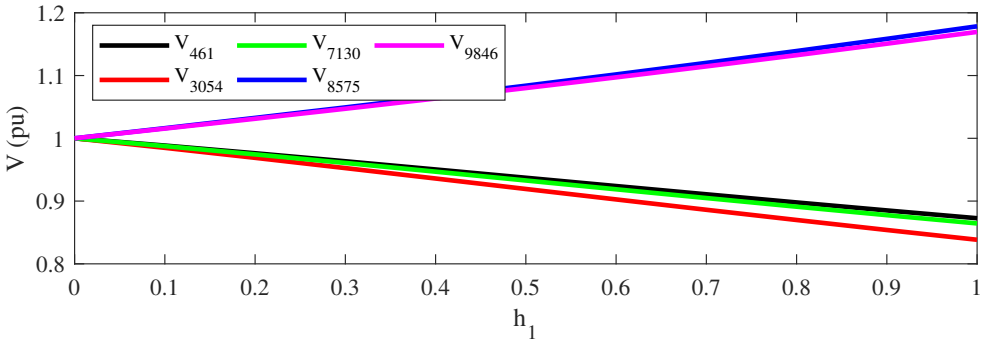

(c) Voltage magnitude, $\delta = 0.12$

Figure 6.5: Evolution of voltage magnitude in some buses of the 13,659-bus system for δ equal to 0.01, 0.1 and 0.12

6.7 Experiments on a very large-scale model

This subsection describes tests and results on the 70,000-bus test system [46, 47].

Again, simulations were assessed with the NR method by considering the initial estimate given in MATPOWER's databank and an estimation of the flat start type imposed in this

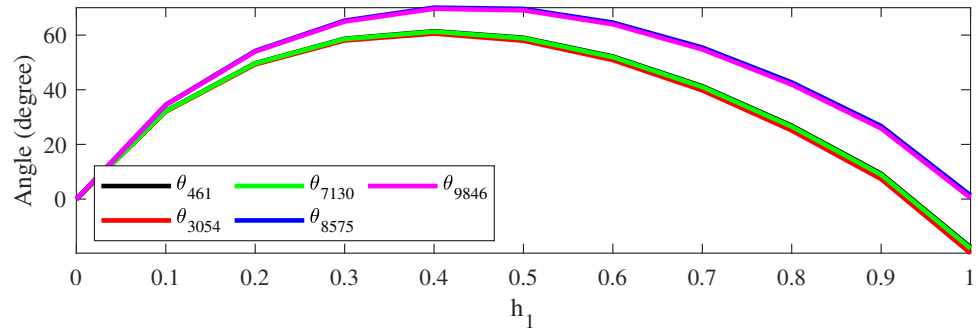

(a) Voltage angle, $\delta = 0.01$

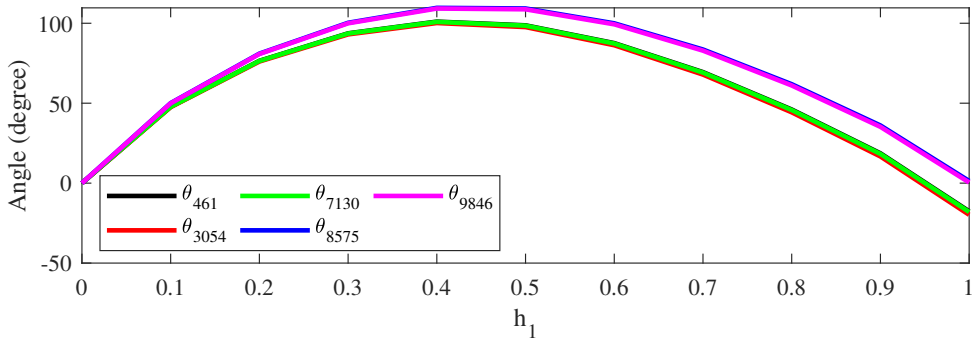

(b) Voltage angle, $\delta = 0.1$

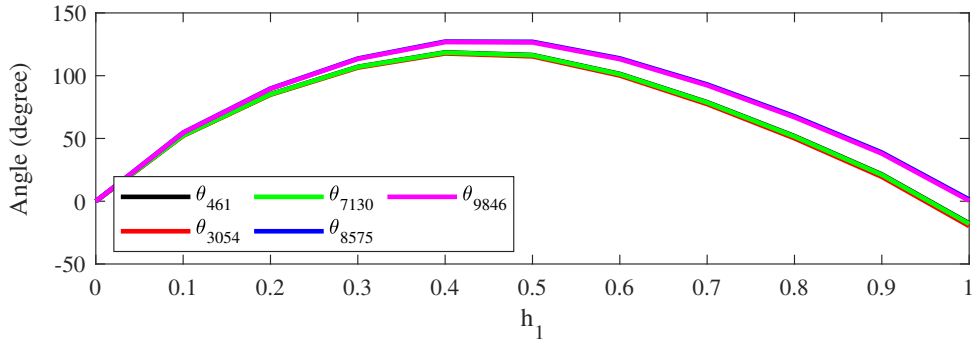

(c) Voltage angle, $\delta = 0.12$

Figure 6.6: Evolution of voltage angle in some buses of the 13,659-bus system for δ equal to 0.01, 0.1 and 0.12

work. For the first situation, the NR method converged to the solution with 6 iterations. Fig. 6.8 is a plot illustration of the initial state values (voltage magnitude and phase angle) and the final solution. Note that the initial states have values closer to the solution. However, for the second situation, the convergence failed, requiring another strategy to solve the problem. Then, the GSH-NR method was applied for this divergent case.

The homotopy-based method was employed by using step 0.1 for h_1. This demands solving 11 times a standard PFP via the NR method with a mean of 3 to 4 iterations to converge each iteration. However, this is the price paid to solve the problem, which could not be resolved numerically through the standard NR method and other technique investigated in Tab. 6.3.

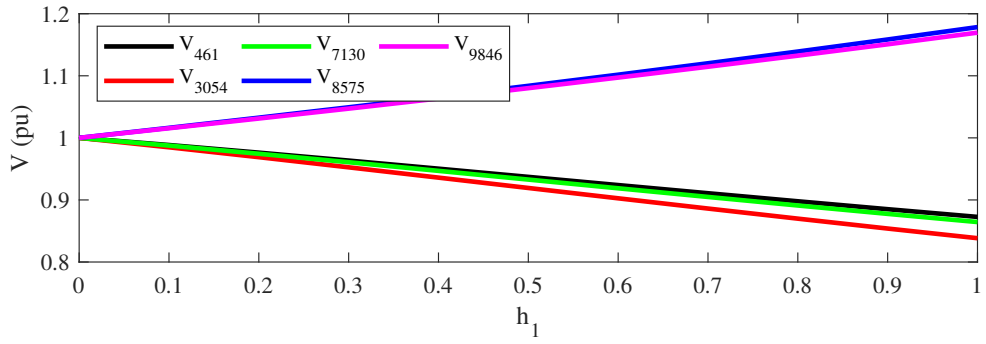

(a) Voltage magnitude

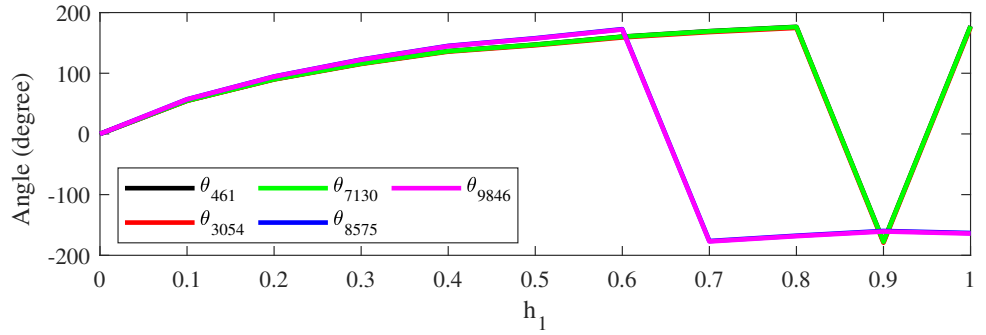

(b) Voltage angle

Figure 6.7: Evolution of voltage in some buses of the 13,659-bus system for $\delta = 0.13$

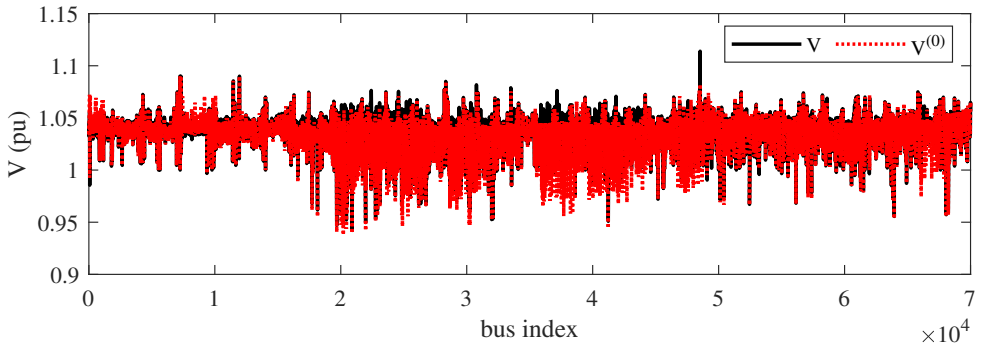

(a) Voltage magnitude

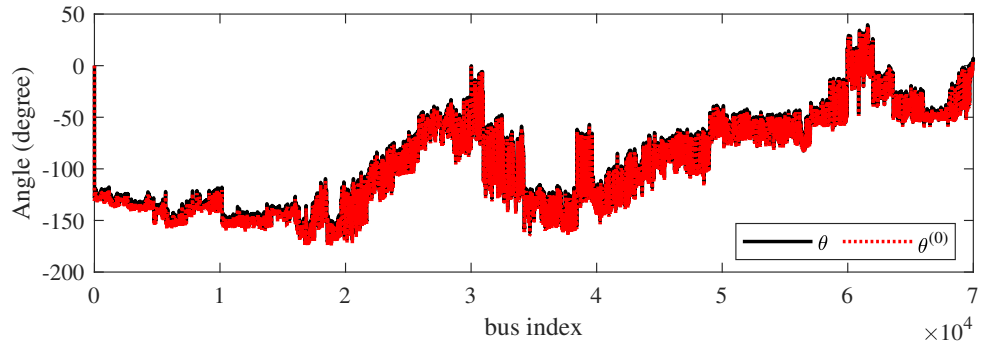

(b) Voltage angle

Figure 6.8: Initial estimation and final states for the 70,000-bus system

In contrast to the 13,659-bus model, the parameter δ for the 70,000-bus system was adopted for a large range of values without restrictions. This way, it is adequate for $\delta \leq 1.0$. An explanation for this is the reduced number of interconnections at the high voltage side neighborhood of the slack bus $(\#30902)$ and the adequate capacity of the links to support elevated changes at the interconnections. While the latter has only 2 links connecting the high voltage side, as can be seen from Fig. 6.9.b, the former has 26 links, as can be seen from Fig. 6.9.a. Both systems have just 1 direct connection (transformer device) with the slack bus (low voltage). Fig. 6.10 and 6.11 depicts plots for values 0.1 and 1.0 for δ. The magnitude and angle of voltages at the index of buses $\#461$, $\#3054$, $\#8575$, $\#9846$, and $\#50000$ are observed. Note that both voltage magnitudes and phase angles are practically insensitive to changes in this parameter. Despite the large variation in the phase angles, they occur in continuous form, indicating that the homotopy process is adequate for searching the operation point, even for large changes in the phase angle.

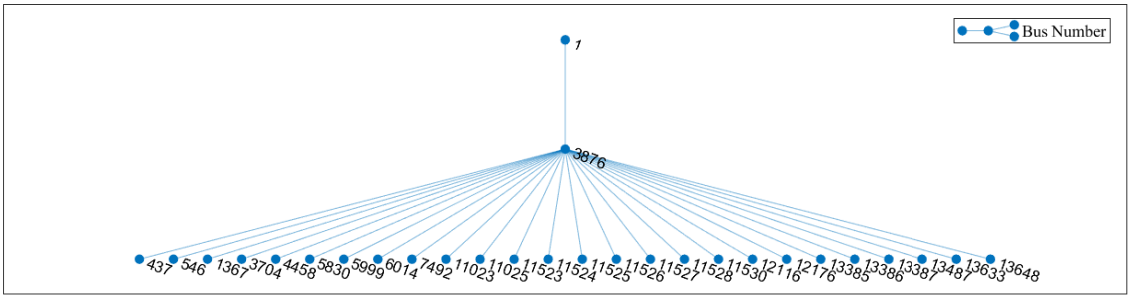

(a) Buses neighborhood near by slack bus $(\#1)$ at 13659-bus system

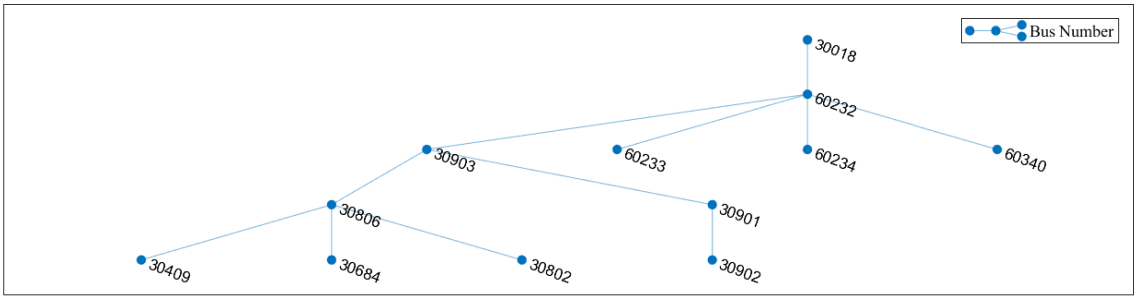

(b) Buses neighborhood near by slack bus $(\#30902)$ at 70k-bus system

Figure 6.9: Buses near by slack bus

6.7.1 Execution time

This subsection highlights the execution time (CPU time) for running the scripts associated with the 9-, 13,659- and 70,000-bus system used in the simulations. Each simulation was repeated 100 times, and the mean time for one simulation was obtained. Table 6.5 shows the mean CPU time for a given system considering the value of the parameter δ to perform

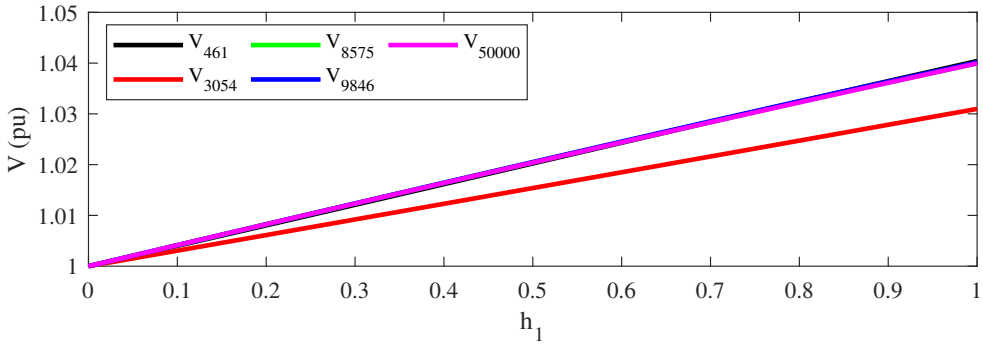

(a) Voltage magnitude, $\delta = 0.1$

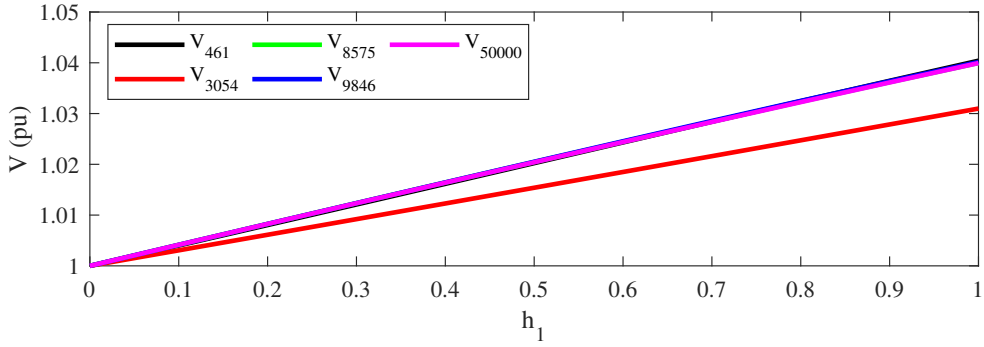

(b) Voltage magnitude, $\delta = 1.0$

Figure 6.10: Evolution of voltage magnitude in some buses for the 70,000-bus system considering δ equal to 0.1 and 1.0

simulations by using the GSH-NR method. Using the same step 0.1 for the homotopy parameter, a standard PFP is solved 11 times to reach the final solution at $h_1 = 1$. In general, for a given model, the mean time is approximately the same independent of the δ value adopted. Additionally, assuming that the PFP is convergent, only 3 iterations are required to obtain the solution at a particular parameter h_1 (solution obtained by a standard NR method). This is justified because the solution obtained for a previous step of h_1 approximates well that of the next step.

Table 6.5: Mean CPU Time for running the experiments according to the model size and the δ value.

CASE	9			13659pegase				ACTIVSg70k
δ	0.01	0.10	0.5	0.01	0.10	0.12	0.13	0.1
t_{CPU} (s)	0.0803	0.0880	0.0816	9.7405	9.7502	9.7458	10.5538	421.3

Table 6.6 shows results for the two most significant models, including details of the execution time for intermediate states along the homotopy process. Also, for illustration, it is indicated the runtime for the standard NR method using the initial estimate from MATPOWER. We can observe that the homotopy-based method needs several steps to move from the initial solution to the final one. However, it reaches a solution from an initial estimate of type

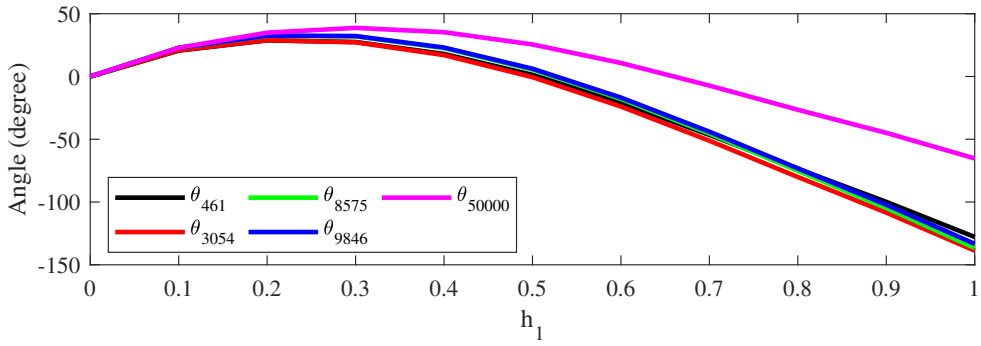

(a) Voltage angle, $\delta = 0.1$

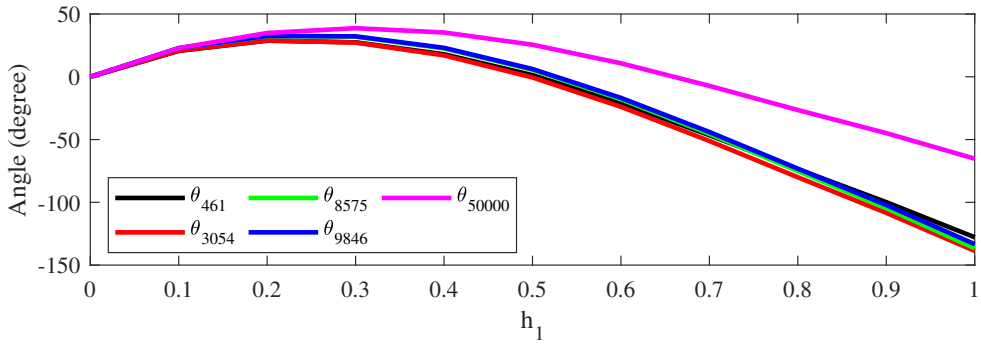

(b) Voltage angle, $\delta = 1.0$

Figure 6.11: Evolution of voltage angle in some buses for the 70,000-bus system considering δ equal to 0.1 and 1.0

flat start. The NR method converges only by using an estimate very close to the solution. Therefore, even with the computational burden about eight times the cost of the standard NR solver, the performance of the homotopy-based method is well adequate.

Table 6.6: Execution time in seconds for computation of a homotopy path with a given step Δh_1 and the partial CPU time required at an intermediate state

CASE		Homotopy											NR
13659 pegase	h_1	0.0	0.1	0.2	0.3	0.4	0.5	0.6	0.7	0.8	0.9	1.0	-
	$iter.$	-	5	4	4	4	4	4	4	4	4	4	5
	t_{cpu}	-	0.4080	0.2995	0.3008	0.2970	0.3080	0.3040	0.3080	0.3070	0.3160	0.2950	0.4425
ACTIVS g70k	h_1	0.0	0.1	0.2	0.3	0.4	0.5	0.6	0.7	0.8	0.9	1.0	-
	$iter.$	-	5	4	4	4	4	4	4	4	4	5	6
	t_{cpu}	-	2.5220	1.9930	1.9520	2.0050	2.0040	1.9950	1.9570	1.9600	1.9870	2.4550	3.0720

h_1: Homotopy parameter; $iter.$: Iteration number; t_{cpu}: Computer burden in seconds.

6.7.2 Experiments considering reactive power operational limits

To determine the ability of the PFP to deal with reactive operational limits in generators, experiments were carried out specifically for this purpose. With no loss of content, as the 13,659- and 70,000-bus models are the most complex to address because of their sizes, only their results are presented.

To simulate the effect of operational limit inclusion, we use a traditional method that is based on the iterative computation of the PFP solution, followed by the monitoring of the reactive power generator operational limits [40, 42]. Following this strategy, a PFP is solved, and in the sequence, whether the operational limits of all generators are satisfied. If any limit is violated, the PV bus associated with the violated limit is converted to a PQ bus, and the PFP is resolved again. In the sequence, we verify whether the PV buses that were converted to PQ continue with their reactive power out of the limits. Case positive, the conversion to PQ bus is kept; otherwise, the PQ bus is transformed back to PV. This procedure is repeated until a result for convergence/failure is obtained. For the first iteration, the calculation is carried out with all operational limits free. The GSH-NR method with flat start initialization is applied since the straightforward application of the NR method with flat start is divergent for all system, unless the 9- and 300-bus model. From the solution, in case of violation of limits, they are separated to be provided the conversion of PV to PQ buses. In the subsequent iterations, for all test system used in this work, only the NR method is used because the solution associated with the previous iteration is closer to the result for the current iteration. All simulations were executed using MATPOWER's framework with the code properly adapted. To track the impact of the modification on the limits, we have observed the generation results in the slack bus.

The 13,659-bus system had its first limit-based iteration resolved by considering $\delta = 0.1$ and was applied as a scaling factor to the links connecting the low voltage and high voltage of the slack bus. The generation at the slack bus with a free limit at all generation buses was 0.7687 pu and 0.1581 pu for the active and reactive power, respectively. It was detected that only 1 upper limit of a generator had been exceeded. In the iteration performed in the sequence considering the exceeded limit, the generation in the slack bus was 0.7713 pu and 0.1583 pu for the active and reactive power, respectively. After this limit-based iteration, all constraints were met this time.

The 70,000-bus model presented much more exceeded limits. This method requires more iterations at the limit-based loop to reach convergence. The first iteration (with limit free) and GSH-NR method was performed considering $\delta = 0.1$. The generation at the slack bus was 13.2478 pu and 0.7668 pu, for the active and reactive power, respectively. However, a total of 4,588 limits (2,190 upper and 2,398 lower) were violated. In the second iteration, after correction of limits, the generation of the slack bus was 14.2054 pu and 0.9828 pu for the active and reactive power, respectively. At the end of the iteration, a total of 700 limits were exceeded (422 upper and 278 lower). For the third iteration, the slack bus provided 14.5396 pu and 1.0614 pu, respectively, for the active and reactive power, but 200 limits (143 upper and 57 lower) were still exceeded. In the fourth iteration, only 11 limits were violated, and the generation at the slack bus was 14.5722 pu and 1.0692 pu, respectively, for the active and reactive power. Finally, in the fifth iteration, no more limits were exceeded, and the final generation for the active and reactive power at the slack bus was 14.5726 pu and 1.0693 pu, respectively. The Tab. 6.7 summarize the steps to reach the correct answer

considering the reactive limits.

Table 6.7: Results considering the reactive limits

Case	Violated Limits	Limits free	Limits considered			
		1^{st}	2^{nd}	3^{th}	4^{th}	5^{th}
13659 pegase	Upper:	1	0	-	-	-
	Lower:	0	0	-	-	-
	P_s:	0.7687	0.7713	-	-	-
	Q_s:	0.1581	0.1583	-	-	-
	$\#iter$:	-	3	-	-	-
ACTIVS g70k	Upper:	2190	422	143	8	0
	Lower:	2398	278	57	3	0
	P_s:	13.2478	14.2054	14.5396	14.5722	14.5726
	Q_s:	0.7668	0.9828	1.0614	1.0692	1.0693
	$\#iter$:	-	4	3	3	2

Note that for each iteration in which the limits are modified, the generation at the slack bus is augmented. Additionally, the standard NR method for the limit-based iteration generally converges with 2 or 3 iterations, confirming that the results between one iteration and the other are closer.

6.8 Conclusion of this chapter

In this chapter, the method GSH-NR was tested in different power systems network to evaluate the convergence effectiveness and computational cost efficiency as well as number of iterations. The systems `case3.m`, `case9.m` and `case300.m` was used just to illustrate the GSH-NR since they are well-conditioned cases. The other ones are considered ill-conditioned systems and large-scale systems. They converged to the right solution starting from flat start point. To validate the results others techniques were simulated, as BE, RK4 and IH. Experiments with these techniques they do not reach convergence starting from the flat initial guess. The computational burden was presented to demonstrate that the GSH-NR has additional burden due to the need to run NR in different steps along the homotopy path. The experiments showed that the implemented algorithm considers the reactive power limits imposed by the generators of the systems, which is practical for the solution of large-scale power systems.

Chapter 7

Conclusion

7.1 General Conclusion

This work presented a homotopy-based method to calculate the solution of a power flow problem. We denominated Guided Solution Homotopy - Newton-Raphson (GSH-NR) solver, since it uses the standard NR method to determine the solution along with the homotopy path. The proposed technique search a solution through an iterative homotopy path, where a partial fictitious network is inserted in the beginning of the process and removed gradually depending on two homotopy parameters.

The proposed method

- is based on the control of a fictitious compensation network which is inserted at the first step of the homotopy process, being their parameters designed to allow a flat start type initial estimate for the PFP; also, producing a trivial solution equal to the initial estimate;
- worked properly for large-scale and well- and ill-conditioned power system models, being tested for model of practical power system size, as the 70,000-bus synthetic USA test system [46, 47];
- is fully compatible with the MATPOWER's case databank and this way it can be implemented in the kernel of this well-known software through single adaptations;
- allows for solving problems which the standard NR and other methods are unable to resolve starting from an initial estimate of flat start type;
- employs the polar representation form for voltages and power mismatches, being that along with the homotopy path different from the last state of the path, the tolerance for convergence of the classical NR method can be relaxed, e.g. for 10^{-2} pu, which is well smaller than the usual 10^{-8} pu.

Simulations were carried out by using other approaches, as the implicit Continuous Newton's method philosophy (implicit and explicit form), and a power injection homotopy-based method. The GSH-NR have presented superior performance compared to other techniques studied in this work.

Other tests also considered situations for reactive operational limits in generators. The first limit-based iteration is carried out free of limits and by using the GSH-NR solver. However, we have observed in our tests that the standard NR method can be used after evaluating the first limit-based iteration without the need to implement a new homotopy process.

To achieve the final results, this work considered an introductory part emphasizing the motivation and highlighting the main objectives of the work. Following, a chapter was dedicated to a basic bibliographic review of works involving the dissertation theme. An introduction of the load flow problem and the methods of solving the problem was included in the third chapter. Besides the traditional approach by the NR method, other ones based on the called Newton's continuous method were discussed. It was explained how the homotopy problem was addressed, going through the definition of its formulation from a fictitious compensation network. Finally, several experiments were carried out considering miscellaneous test systems, with different characteristics such as well- or ill-conditioned profile and also small and large-scale size.

7.2 Future Works

The homotopy method applied to the study of power flow allows a broadening of the approach, as well as simulating different possible scenarios within the context of power systems. Among the ideas for future works can be cited the following:

- investigate other forms of generating and setting fictitious network compensation;
- test the methodology with other modeling networks as isolated power system (microgrid);
- simulate real scenarios under contingencies;
- extend the methodology to cover the PFP for distribution systems involving different sources of generations, loads, and transformer configurations;
- test other more robust algorithms for solving ill-conditioned cases instead of NR for the intermediate steps of the homotopy process and test the efficiency for large scale systems.

Bibliography

[1] EPE. *Estudos do Plano Decenal de Expansão de Energia 2031 - Demanda de Eletricidade*. Empresa de Pesquisa Energética - EPE / Ministério de Minas e Energia, 2021. 19 p. Available: <https://www.epe.gov.br/sites-pt/publicacoes-dados-abertos/publicacoes/PublicacoesArquivos/publicacao-490/topico-522/Caderno de Demanda de Eletricidade - PDE 2030 (1).pdf>.

[2] WU, D.; WANG, B. Holomorphic Embedding Based Continuation Method for Identifying Multiple Power Flow Solutions. *IEEE Access*, Institute of Electrical and Electronics Engineers Inc., Laboratory for Information and Decision Systems, Massachusetts Institute of Technology, Cambridge, MA, United States, v. 7, p. 86843–86853, 2019. ISSN 2169-3536. Available: <https://ieeexplore.ieee.org/document/8747482/>.

[3] RAO, S. et al. The Holomorphic Embedding Method Applied to the Power-Flow Problem. *IEEE Transactions on Power Systems*, Institute of Electrical and Electronics Engineers Inc., School of Electrical Computer and Energy Engineering, Arizona State University, Tempe, AZ 85287, United States, v. 31, n. 5, p. 3816–3828, sep 2016. ISSN 0885-8950. Available: <http://ieeexplore.ieee.org/document/7352383/>.

[4] KUNDUR, P. *Power System Stability and Control*. 1st. ed. New York: McGraw-Hill, EPRI, Power Engineering Series, 1994.

[5] TINNEY, W.; HART, C. Power Flow Solution by Newton's Method. *IEEE Transactions on Power Apparatus and Systems*, PAS-86, n. 11, p. 1449–1460, Nov. 1967. ISSN 0018-9510. Available: <http://ieeexplore.ieee.org/document/4073219/>.

[6] ALVES, G. O.; PEREIRA, J. L. R.; Passos Filho, J. A. A new unbalanced three-phase governor power flow formulation based on the current injections method. *International Journal of Electrical Power and Energy Systems*, Elsevier, v. 123, n. 106184, p. 1–13, 2020. ISSN 01420615. Available: <https://doi.org/10.1016/j.ijepes.2020.106184>.

[7] MILANO, F. *Power System Modelling and Scripting*. Spain: Springer Berlin Heidelberg, 2010. 556 p. ISSN 1612-1287. ISBN 978-3-642-13668-9. Available: <http://link.springer.com/10.1007/978-3-642-13669-6>.

[8] MILANO, F. Continuous Newton's Method for Power Flow Analysis. *IEEE Transactions on Power Systems*, v. 24, n. 1, p. 50–57, 2009. ISSN 0885-8950. Available: <http://ieeexplore.ieee.org/document/4682629/>.

[9] HU, S. T. *Homotopy theory*. Wayne State University, Detroit, MI: Academic press, 1959.

[10] LIAO, S. *Homotopy analysis method in nonlinear differential equations*. Beijing: Springer, 2012.

[11] DAVIDENKO, D. F. On the approximate solution of systems of nonlinear equations. *Ukr. Mat. Zh*, v. 5, n. 2, p. 196–206, 1953.

[12] CHEN, J.-F.; CHEN, H.-c.; HUANG, C.-l. The uniqueness of the local minimum for power economic dispatch problems. *Electric Power Systems Research*, v. 32, n. 3, p. 187–193, mar 1995. ISSN 03787796. Available: <https://linkinghub.elsevier.com/retrieve/pii/037877969400914P>.

[13] TOLIKAS, M.; TRAJKOVIC, L.; ILIC, M. Homotopy methods for solving decoupled power flow equations. In: *[Proceedings] 1992 IEEE International Symposium on Circuits and Systems*. Laboratory for Electromagnetic and Electronic Systems, Massachusetts Institute of Technology, Cambridge, MA 02139, United States: IEEE, 1992. v. 6, p. 2833–2839. ISBN 0-7803-0593-0. Available: <http://ieeexplore.ieee.org/document/230609/>.

[14] CHIANG, H.-D. et al. Homotopy-Enhanced Power Flow Methods for General Distribution Networks With Distributed Generators. *IEEE Transactions on Power Systems*, School of Electrical and Computer Engineering, Cornell University, Ithaca, NY 14853, United States, v. 29, n. 1, p. 93–100, jan 2014. ISSN 0885-8950. Available: <http://ieeexplore.ieee.org/document/6588949/>.

[15] CHIANG, H.-D.; WANG, T. Novel Homotopy Theory for Nonlinear Networks and Systems and Its Applications to Electrical Grids. *IEEE Transactions on Control of Network Systems*, School of Electrical and Computer Engineering, Cornell University, Ithaca, NY 14853, United States, v. 5, n. 3, p. 1051–1060, sep 2018. Available: <https://ieeexplore.ieee.org/document/7862794/>.

[16] PANDEY, A. et al. Robust Convergence of Power Flow Using TX Stepping Method with Equivalent Circuit Formulation. In: *2018 Power Systems Computation Conference (PSCC)*. IEEE, 2018. p. 1–7. ISBN 978-1-910963-10-4. Available: <https://ieeexplore.ieee.org/document/8442680/>.

[17] MURRAY, W.; De Rubira, T. T.; WIGINGTON, A. Improving the robustness of Newton-based power flow methods to cope with poor initial points. In: *2013 North American Power Symposium (NAPS)*. IEEE, 2013. p. 1–6. ISBN 978-1-4799-1255-1. Available: <http://ieeexplore.ieee.org/document/6666905/>.

[18] YANG, X.; ZHOU, X. Application of asymptotic numerical method with homotopy techniques to power flow problems. *International Journal of Electrical Power and Energy Systems*, Elsevier Ltd, v. 57, p. 375–383, 2014. Available: <http://dx.doi.org/10.1016/j.ijepes.2013.12.014>.

[19] JEREMINOV, M. et al. Robust and Efficient Power Flow Convergence with G-min Stepping Homotopy Method. In: *2019 IEEE International Conference on Environment and Electrical Engineering and 2019 IEEE Industrial and Commercial Power Systems Europe (EEEIC / I&CPS Europe)*. IEEE, 2019. p. 1–6. ISBN 978-1-7281-0653-3. Available: <https://ieeexplore.ieee.org/document/8783295/>.

[20] PARK, S. et al. Homotopy Method for Finding the Global Solution of Post-contingency Optimal Power Flow. In: *2020 American Control Conference (ACC)*. Denver, CO, USA: IEEE, 2020. v. 2020-July, p. 3126–3133. ISBN 978-1-5386-8266-1. ISSN 07431619. Available: <https://ieeexplore.ieee.org/document/9147711/>.

[21] PANDEY, A.; AGARWAL, A.; PILEGGI, L. Incremental Model Building Homotopy Approach for Solving Exact AC-Constrained Optimal Power Flow. In: *Proceedings of the Annual Hawaii International Conference on System Sciences*. ECE, Carnegie Mellon University, United States: Cornell University, 2020. p. 3273–3282. Available: <http://arxiv.org/abs/2011.00587>.

[22] ZÁRATE-MIÑANO, R.; Flores Burgos, A.; CARRIÓN, M. Analysis of different modeling approaches for integration studies of plug-in electric vehicles. *International Journal of Electrical Power and Energy Systems*, Elsevier, v. 114, n. February 2019, p. 105398, 2020. ISSN 01420615. Available: <https://doi.org/10.1016/j.ijepes.2019.105398>.

[23] MOLZAHN, D. K. Computing the Feasible Spaces of Optimal Power Flow Problems. *IEEE Transactions on Power Systems*, Energy Systems Division, Argonne National Laboratory, Lemont, IL 6043, United States, v. 32, n. 6, p. 4752–4763, nov 2017. Available: <http://ieeexplore.ieee.org/document/7879340/>.

[24] AGARWAL, A.; PILEGGI, L. Large Scale Multi-Period Optimal Power Flow with Energy Storage Systems Using Differential Dynamic Programmingind. *IEEE Transactions on Power Systems, Early Access*, Electrical and Computer Engineering, Carnegie Mellon University, 6612 Pittsburgh, Pennsylvania, United States, p. 1–10, Sep. 2021. ISSN 0885-8950. Available: <https://ieeexplore.ieee.org/document/9549701/>.

[25] CHANDRA, S.; MEHTA, D.; CHAKRABORTTY, A. Equilibria analysis of power systems using a numerical homotopy method. In: *2015 IEEE Power & Energy Society General Meeting*. IEEE, 2015. p. 1–5. ISBN 978-1-4673-8040-9. Available: <http://ieeexplore.ieee.org/document/7285823/>.

[26] BIE, P. et al. Toward online multi-period power dispatch with AC constraints and renewable energy. *IET Generation, Transmission Distribution*, State Key Laboratory of

Advanced Electromagnetic Engineering and Technology, School of Electrical and Electronic Engineering, Huazhong University of Science and Technology, Wuhan, Hubei Province, China, v. 12, n. 14, p. 3502–3509, aug 2018. ISSN 1751-8687. Available: <https://onlinelibrary.wiley.com/doi/10.1049/iet-gtd.2018.0164>.

[27] BIE, P. et al. Online Multiperiod Power Dispatch With Renewable Uncertainty and Storage: A Two-Parameter Homotopy-Enhanced Methodology. *IEEE Transactions on Power Systems*, State Key Laboratory of Advanced Electromagnetic Engineering and Technology, School of Electrical and Electronic Engineering, Huazhong University of Science and Technology, Wuhan, 430074, China, v. 33, n. 6, p. 6321–6331, Nov. 2018. ISSN 0885-8950. Available: <https://ieeexplore.ieee.org/document/8341512/>.

[28] SILVA, A. L.; FREITAS, F. D. Investigation Study on the Voltage Stability Status of a Power Flow Problem Solution. In: *2021 Workshop on Communication Networks and Power Systems (WCNPS)*. IEEE, 2021. p. 1–6. ISBN 978-1-6654-1078-6. Available: <https://ieeexplore.ieee.org/document/9626316/>.

[29] BURGOS, A. F.; ZARATE-MINANO, R.; CARRION, M. Combining quasi-static models and homotopy techniques for loading margin computation. In: *2017 IEEE Central America and Panama Student Conference (CONESCAPAN)*. IEEE, 2017. p. 1–6. ISBN 978-1-5386-2024-3. Available: <http://ieeexplore.ieee.org/document/8277598/>.

[30] NGUYEN, H. D.; TURITSYN, K. Voltage Multistability and Pulse Emergency Control for Distribution System With Power Flow Reversal. *IEEE Transactions on Smart Grid*, Department of Mechanical Engineering, Massachusetts Institute of Technology, Cambridge, MA 02139, United States, v. 6, n. 6, p. 2985–2996, nov 2015. ISSN 1949-3053. Available: <http://ieeexplore.ieee.org/document/7093184/>.

[31] KETTNER, A. M.; PAOLONE, M. Performance assessment of kron reduction in the numerical analysis of polyphase power systems. In: *2019 IEEE Milan PowerTech, PowerTech 2019*. École Polytechnique Fédérale de Lausanne (EPFL), Lausanne, Vaud, Switzerland: IEEE Xplore, 2019. Available: <https://ieeexplore.ieee.org/document/8810904/>.

[32] GLOVER, J. D.; SARMA, M. S.; OVERBYE, T. J. *Power system analysis & design*. 5th. ed. Stamford, USA: Cengage Learning, 2012.

[33] QIN, N. *Voltage control in the future power transmission systems*. Denmark: Springer, 2017. ISBN 978-3-319-69886-1.

[34] STEVENSON, W. D. *Elementos de análise de sistemas de potência*. 2nd. ed. São Paulo: McGraw-Hill do Brasil, 1986.

[35] TOSTADO, M.; KAMEL, S.; JURADO, F. Several robust and efficient load flow techniques based on combined approach for ill-conditioned power systems. *International*

Journal of Electrical Power and Energy Systems, Elsevier, v. 110, n. March, p. 349–356, 2019. Available: <https://doi.org/10.1016/j.ijepes.2019.03.035>.

[36] MILANO, F. Implicit Continuous Newton Method for Power Flow Analysis. *IEEE Transactions on Power Systems*, v. 34, n. 4, p. 3309–3311, jul 2019. ISSN 0885-8950. Available: <https://ieeexplore.ieee.org/document/8698293/>.

[37] ZIMMERMAN, R. D.; MURILLO-SANCHEZ, C. E. *Matpower*. 2020. Available: <https://matpower.org>.

[38] WATSON, L. T. Globally convergent homotopy methods: A tutorial. *Applied Mathematics and Computation*, v. 31, n. 8, p. 369–396, may 1989. ISSN 00963003. Available: <https://linkinghub.elsevier.com/retrieve/pii/009630038990129X>.

[39] MACHOWSKI, J. et al. *Power system dynamics: stability and control*. 3rd. ed. Hoboken, NJ, USA: John Wiley & Sons Ltd, 2020.

[40] ZIMMERMAN, R. D.; MURILLO-SANCHEZ, C. E.; THOMAS, R. J. MATPOWER: Steady-State Operations, Planning, and Analysis Tools for Power Systems Research and Education. *IEEE Transactions on Power Systems*, v. 26, n. 1, p. 12–19, feb 2011. ISSN 0885-8950. Available: <http://ieeexplore.ieee.org/document/5491276/>.

[41] JEREMINOV, M. et al. Evaluating Feasibility Within Power Flow. *IEEE Transactions on Smart Grid*, IEEE, v. 11, n. 4, p. 3522–3534, jul 2020. ISSN 1949-3053. Available: <https://ieeexplore.ieee.org/document/8960553/>.

[42] ZIMMERMAN, R. D.; MURILLO-SANCHEZ, C. E. *Matpower (Version 6.0) [Software]*. 2016. Available: <https://matpower.org>.

[43] IEEE. PES PGLib-OPF Task Force - The Power Grid Library for Benchmarking AC Optimal Power Flow Algorithms. p. 1–17, aug 2021. Available: <http://arxiv.org/abs/1908.02788>.

[44] JOSZ, C. et al. AC Power Flow Data in MATPOWER and QCQP Format: iTesla, RTE Snapshots, and PEGASE. arXiv, p. 1–7, mar 2016. Available: <http://arxiv.org/abs/1603.01533>.

[45] FLISCOUNAKIS, S. et al. Contingency Ranking With Respect to Overloads in Very Large Power Systems Taking Into Account Uncertainty, Preventive, and Corrective Actions. *IEEE Transactions on Power Systems*, v. 28, n. 4, p. 4909–4917, nov 2013. ISSN 0885-8950. Available: <https://ieeexplore.ieee.org/document/6488772/>.

[46] BIRCHFIELD, A. B. et al. Grid Structural Characteristics as Validation Criteria for Synthetic Networks. *IEEE Transactions on Power Systems*, v. 32, n. 4, p. 3258–3265, Jul. 2017. ISSN 0885-8950. Available: <http://ieeexplore.ieee.org/document/7725528/>.

[47] BIRCHFIELD, A. B.; XU, T.; OVERBYE, T. J. Power Flow Convergence and Reactive Power Planning in the Creation of Large Synthetic Grids. *IEEE Transactions on Power Systems*, v. 33, n. 6, p. 6667–6674, Nov. 2018. ISSN 0885-8950. Available: <https://ieeexplore.ieee.org/document/8333771/>.